

Sequence of pseudo-equilibria describes the long-time behaviour of the NNLIF model with large delay

María J. Cáceres* & José A. Cañizo† & Alejandro Ramos-Lora‡
Department of Applied Mathematics & IMAG
University of Granada

Abstract

There is a wide range of mathematical models that describe populations of large numbers of neurons. In this article, we focus on nonlinear noisy leaky integrate and fire (NNLIF) models that describe neuronal activity at the level of the membrane potential. We introduce a sequence of novel states, which we call *pseudo-equilibria*, and give evidence of their defining role in the behaviour of the NNLIF system when a significant synaptic delay is considered. The advantage is that these states are determined solely by the system's parameters and are derived from a sequence of firing rates that result from solving a recurrence equation. We propose a new strategy to show convergence to an equilibrium for a weakly connected system with large transmission delay, based on following the sequence of pseudo-equilibria. Unlike direct entropy dissipation methods, this technique allows us to see how a large delay favours convergence. We present a detailed numerical study to support our results. This study helps understand, among other phenomena, the appearance of periodic solutions in strongly inhibitory networks.

*caceresg@ugr.es

†canizo@ugr.es

‡ramoslora@ugr.es

Contents

1	Introduction	2
2	Firing rate and pseudo-equilibria sequences	8
3	Convergence to equilibrium along the pseudo equilibria sequence for weakly connected networks	17
4	Numerical results: Global perspective on the long-time behaviour of the delayed NNLIF model	25
5	Conclusions	37
A	Appendix: Auxiliary calculations	39

1 Introduction

Over the past few decades, a diverse range of research has emerged in the realm of partial differential equation (PDE) systems to model populations of large numbers of neurons. Depending on the variables taken into account to describe the activity of neurons, several families of PDE have been studied: Fokker-Planck equations including voltage and conductance variables [1–4]; Fokker-Planck equations for uncoupled neurons [5, 6]; population density models of integrate and fire neurons with jumps [7–10]; age structured equations (time elapsed models) [11–13] which are derived as mean-field limits of Hawkes processes [14, 15], McKean-Vlasov equations [16, 17], which are the mean-field equations of a large number of neurons described by the Fitzhugh-Nagumo equation [18], etc.

This article is devoted to the *nonlinear noisy leaky integrate and fire (NNLIF) neuronal system*, which is one of the simplest PDE models [7, 19–23]. We focus on its mesoscopic/macroscopic description through mean-field Fokker-Planck type equations [24–32], although it has also been studied at the microscopic level, using stochastic differential equations (SDE) [33–35]. Despite their simplicity, and the extensive scientific output devoted to them, fundamental questions remain about their long-term behaviour. The aim of this article is to contribute to the understanding of this issue. Specifically, we give evidence that the behaviour of the NNLIF model with large delay is determined by a simple discrete system, which gives us a sequence of novel states, that we call *pseudo-equilibria sequence*. The advantage of the discrete system lies in its simplicity: for instance, it allows for quick simulations that provide accurate information about the NNLIF system. We can rapidly study issues such as the long-term behavior of the system, the estimated time to approach equilibrium, whether the system tends toward a steady state, the possible appearance of periodic solutions or *plateau states*, etc., all in terms of the system parameters.

We will first give a short introduction to the model, and then give our main results. We present the microscopic and mesoscopic descriptions of the NNLIF models.

Stochastic NNIF neuron models. We are interested in describing the membrane potential, which is the potential difference V_i across the cell membrane of the i -th neuron in a group of \mathcal{N} interconnected neurons. A widely used model for this is the *noisy leaky integrate-and-fire model*, which takes into account a simple mechanism for the neuron to approach some natural *resting potential*, V_L , and the effect of the inputs from other neurons. Thus, the evolution on time of the membrane potential for neuron i is given by

$$C_m \frac{dV_i}{dt} = -g_L(V_i - V_L) + I_i(t), \quad (1.1)$$

where C_m is the capacitance of the membrane and g_L is the leak conductance. Equation (1.1) is stochastic, since the term I_i is the sum of all synaptic currents produced by the stochastic spike trains of the C_i neurons connected to neuron i :

$$I_i(t) := \sum_{j=1}^{C_i} \sum_k J_{ij} \delta(t - t_j^k - d).$$

The term $\delta(t - t_j^k - d)$ represents a Dirac delta (in time), modelling the contribution of the k -th spike from the j -th presynaptic neuron. It is modulated by the synaptic strength of the i - j connection, J_{ij} (which may be positive or negative, depending on whether the effect is excitatory or inhibitory, respectively). The constant $d \geq 0$ is the synaptic delay—the time it takes for the effect of a spike to be felt by other neurons.

In addition, this model imposes the condition that whenever a neuron's membrane potential V_i reaches a certain *firing potential* (or *threshold potential* or *firing threshold*) V_F , it discharges by sending a spike over the network, and then V_i is reset to a *reset potential* value V_R . It is always assumed that $V_L < V_R < V_F$.

The following are also common assumptions for this model: networks with sparse random connectivity, i.e. $C/\mathcal{N} \ll 1$; strengths $|J_{ij}| \ll V_F$, i.e., small strengths compared to the threshold potential; and that neurons spike according to stationary, independent Poisson process, with a constant probability ν of emitting a spike per unit time. Under these assumptions we can consider the mean-field limit when $\mathcal{N} \rightarrow \infty$, see [20, 21, 23, 36]. The synaptic current is then approximated by a continuous-in-time stochastic process of Ornstein-Uhlenbeck type with the same mean and variance as the Poissonian spike-train process, so the synaptic current of a typical neuron is

$$I(t)dt \approx b\nu dt + a dB,$$

where B is a Brownian process, and $a > 0$ is the strength of the noise. The parameter b , called the *connectivity parameter*, is an *average* connectivity strength and encodes how excitatory or inhibitory the network is. The case $b = 0$ means that neurons are not connected to each other and the system becomes linear. Otherwise, if $b > 0$ the network is average-excitatory, and if $b < 0$ the network is average-inhibitory.

Therefore, we obtain the stochastic differential equation (SDE) for a typical neuron

$$C_m dV = -g_L(V - V_L) dt + b\nu dt + a dB.$$

By appropriate translation and scaling one can remove the constants C_m , g_L and V_L (see [24, 33, 34, 37]), and obtain the SDE, which we write in the notation we will use throughout the paper:

$$dV = -(V + bN(t - d)) dt + a dB,$$

where $N = N(t)$ is the *mean firing rate* of the network.

The>NNLIF PDE model. The PDE satisfied by the probability distribution of V from the above equation is

$$\partial_t p(v, t) + \partial_v [h(v, N(t-d)) p(v, t)] - a \partial_v^2 p(v, t) = \delta(v - V_R) N(t). \quad (1.2)$$

It requires a given non-negative, integrable initial condition $p(v, 0) = p_0(v) \geq 0$, regular enough for its associated firing rate to exist:

$$N(t) = -a \partial_v p_0(V_F) \text{ for } t \in [-d, 0].$$

This is the PDE we address in this paper, previously studied in many references; see for example [21, 33–35] and the references therein. As described, it arises as the mean-field limit of a large set of \mathcal{N} identical neurons which are connected to each other in a network, when $\mathcal{N} \rightarrow +\infty$. This PDE provides the evolution in time $t \geq 0$ of the probability density $p(v, t) \geq 0$ of finding neurons at voltage $v \in (-\infty, V_F]$. A neuron spikes when its membrane voltage reaches the firing threshold value V_F , discharges immediately after, and has its membrane potential set back to the reset value V_R ($V_R < V_F$), which is described by the right hand side of the equation and the boundary condition $p(V_F, t) = 0$. In addition, the model includes the delay d in synaptic transmission. In this paper we assume the diffusion coefficient $a > 0$ to be constant, and we always take the drift coefficient h to be $h(v, N) := -v + bN$. This makes the system nonlinear since the firing rate $N = N(t)$ must be computed as

$$N(t) := -a \partial_v p(V_F, t) \geq 0 \quad (1.3)$$

so that the total number of neurons $\int_{-\infty}^{V_F} p(v, t) dv$ is conserved. Due to our definition of N in (1.3), and assuming $p(-\infty, t) = 0$, the solution to the related Cauchy problem conserves the total number of neurons:

$$\int_{-\infty}^{V_F} p(v, t) dv = \int_{-\infty}^{V_F} p_0(v) dv, \quad \text{for } t \in [0, T],$$

where $T > 0$ is the maximal time of existence [25, 29, 31].

In general,>NNLIF systems describe the activity of large numbers of neurons in terms of the distribution of the membrane potential. The PDE-based>NNLIF family includes systems with different complexity depending on the neurophysiological properties that are taken into account [38]. In this article we always focus on the nonlinear Fokker-Planck equation (1.2). For the sake of simplicity, we always assume that $\int_{-\infty}^{V_F} p_0(v) dv = 1$ and take a diffusion coefficient $a = 1$.

Stationary states. The probability *stationary states*, *steady states*, or *equilibria*, $p_\infty(v)$, of system (1.2) are non negative solutions to

$$\begin{cases} \partial_v [(-v + bN_\infty) p_\infty(v)] - \partial_v^2 p_\infty(v) = \delta(v - V_R) N_\infty, \\ N_\infty := -\partial_v p_\infty(V_F), \text{ and } \int_{-\infty}^{V_F} p_\infty(v) dv = 1, \end{cases} \quad (1.4)$$

and are given by

$$p_\infty(v) = N_\infty e^{-\frac{(v-bN_\infty)^2}{2}} \int_{\max(v, V_R)}^{V_F} e^{\frac{(w-bN_\infty)^2}{2}} dw. \quad (1.5)$$

The stationary firing rate N_∞ is implicitly given by the requirement of unit mass ($\int_{-\infty}^{V_F} p_\infty(v) dv = 1$), which is translated into the condition $N_\infty I(N_\infty) = 1$, where

$$I(N) := \int_{-\infty}^{V_F} e^{-\frac{(v-bN)^2}{2}} \int_{\max(v, V_R)}^{V_F} e^{\frac{(w-bN)^2}{2}} dw dv. \quad (1.6)$$

Every stationary state corresponds to a solution of the implicit equation $N_\infty I(N_\infty) = 1$ for N_∞ . The number of steady states depends on the connectivity parameter b [24]: for $b \leq 0$ (inhibitory case or the case where neurons are not connected to each other) there is only one, while for $b > 0$ (excitatory case) there is more variety: there is only one if b is small; there are no steady states if b is large; and there are two for intermediate values of b (the existence of at least two can be proved analytically; exactly two are observed numerically).

Known results on the PDE. For the nonlinear Fokker-Planck Equation (1.2) there is a global in time solution if either $d > 0$ [29, 31], or if $d = 0$ and $b \leq 0$ (average-inhibitory and linear cases) [25]. However, for the average-excitatory case ($b > 0$), blow-up of the solution may occur, and in this case the maximal time of existence is given by the first time at which the firing rate $N(t)$ diverges [24, 25]. This is known to happen if there is no transmission delay and the initial condition is sufficiently concentrated around the threshold potential V_F , or if the connectivity parameter b is large enough [31]. The blow-up is avoided if some transmission delay or stochastic discharge potential are considered [26]. The analogous criteria for existence and blow-up phenomena were studied in [33], for the associated microscopic system. Moreover, the notion of physical solutions to the SDE was given in [34] and the authors proved physical solutions are global on time, solutions continue after system synchronization, this is after the blow-up phenomenon. Understanding what “physical solution” may mean for the Fokker-Planck equation is an open problem. It was numerically analysed in [37], and behaviour after the explosion was studied in [39] by a time change of variable which dilates the blow-up time.

Let us give a brief review of the existing results on asymptotic behaviour. Most of the literature on asymptotic behaviour of the model (1.2) is based on the entropy dissipation method (see [24, 26, 27, 29, 40]), considering a standard relative entropy functional to estimate the distance between the solution p and the stationary solution p_∞ . This strategy has given results only for weakly connected networks (small values of the connectivity parameter b), that is, almost linear systems. Recently, approaches based on Doeblin & Harris’s theorems in probability have been used in the study of the asymptotic behaviour of various equations related to neural networks, for both elapsed time [41] and integrate-and-fire models [10, 42]. Again, both strategies (entropy method and Harris-type theorems) seem to be suitable only for nearly linear systems. Results on the long-term behaviour for general connectivity have been recently given in [43] by using a new strategy based on the spectral gap properties of the linearised equation. On the other hand, [29, 31] proved that there are no periodic solutions if b is large enough, $V_F \leq 0$ and a transmission delay is considered. Recently in [32] it was shown that periodic solutions can appear in the average-inhibitory case if a large delay is considered for an approximation of the integrate-and-fire model. Moreover, for the

more realistic model (considering as different populations the excitatory and inhibitory neurons, or neurons with refractory periods) and the stochastic discharge potential model, the results in [26, 28, 30, 44, 45] numerically show periodic solutions.

Main ideas and the pseudo-equilibria sequence. Let us describe the main ideas in the present paper. We wish to examine a discrete sequence determined by the parameters of the nonlinear system (1.2). For a given $N \geq 0$ we define the *pseudo-equilibrium* associated to N as

$$p_{\text{pseudo}}(v) := \tilde{N} e^{-\frac{(v-bN)^2}{2}} \int_{\max(v, V_R)}^{V_F} e^{\frac{(w-bN)^2}{2}} dw, \quad \text{with} \quad \tilde{N} = \frac{1}{I(N)}. \quad (1.7)$$

This is just an equilibrium for the linear version of equation (1.2), where the dependence of h on $N(t-d)$ is “frozen” at a certain value N . The constant \tilde{N} guarantees unit mass: $\int_{-\infty}^{V_F} p_{\text{pseudo}}(v) dv = 1$. The profile p_{pseudo} is an equilibrium of the NNLF system (1.2) if and only if and only if $\tilde{N} = N$, that is, if and only if $NI(N) = 1$.

Our guiding idea is that for a large delay d , the NNLF system (1.2) behaves almost as a linear system in time intervals of length d . Assume that we start with a constant initial condition on $[-d, 0]$, which has a firing rate $N_{0,\infty}$. Then the NNLF system is exactly linear on $[0, d]$; d is large, we expect the solution at $t = d$ to be close to the linear equilibrium associated to a *fixed* firing rate $N_{0,\infty}$, that is, the pseudo-equilibrium associated to a certain firing rate $N_{1,\infty}$. This corresponds to taking $N = N_{0,\infty}$ and $\tilde{N} = N_{1,\infty}$ in (1.7). On the time interval $[d, 2d]$, if on $[0, d]$ the firing rate has remained close to $N_{1,\infty}$, we expect the solution to again behave linearly, and approach another pseudo-equilibrium with firing rate $N_{2,\infty}$. Iterating this we define a sequence of pseudo-equilibria determined solely by the initial value $N_{0,\infty}$ (and the given parameters V_R, V_F, b). We are able to rigorously prove that this sequence represents the behaviour of the system with long delays for the case of small b (see Section 3), but we are unable to do so for general values of b . However, we present strong numerical evidence that this sequence does represent the overall behaviour of the system (cf. Section 4). In particular, this sequence shows periodic behaviour for b negative enough; converges to the stable equilibrium of (1.2) in the region where solutions (1.2) do the same; and approaches a *plateau state* when solutions to (1.2) are expected to do this.

Let us describe this plateau state more closely, since it is also an important evidence for the usefulness of the pseudo-equilibria sequence. Recently, in [37] we numerically observed the formation of a new profile, which describes networks with uniformly distributed membrane potentials between the reset value V_R and the threshold value V_F . We called these states “plateau” distributions. These profiles appear in two situations: 1) strongly connected systems (high connectivity parameter b) with synaptic delay $d > 0$, and 2) systems with $b = V_F - V_R$, without delay ($d = 0$) or with very small transmission delay value. Numerically we observe that plateau states appear to be related to pseudo-equilibria in the following way: Figure 1 shows the comparison of the plateau distributions found for $b = 1.5$ (left plot) and $b = 2.2$ (right plot), with delay transmission, and several pseudo-equilibria. There is a high coincidence between the plateau distributions and the profiles (1.7) as N increases. Furthermore, on the way to the plateau state, the dynamics of the particle system appears to pass through pseudo-equilibria of the form (1.7) as N increases. For $b = 1.5$ the system (1.2) has two steady states, and it can evolve towards a plateau distribution (shown on the left plot) if the

initial condition is far from the stationary state with lowest firing rate. For $b = 2.2$ there are no stationary solutions and the system evolves towards a plateau distribution.

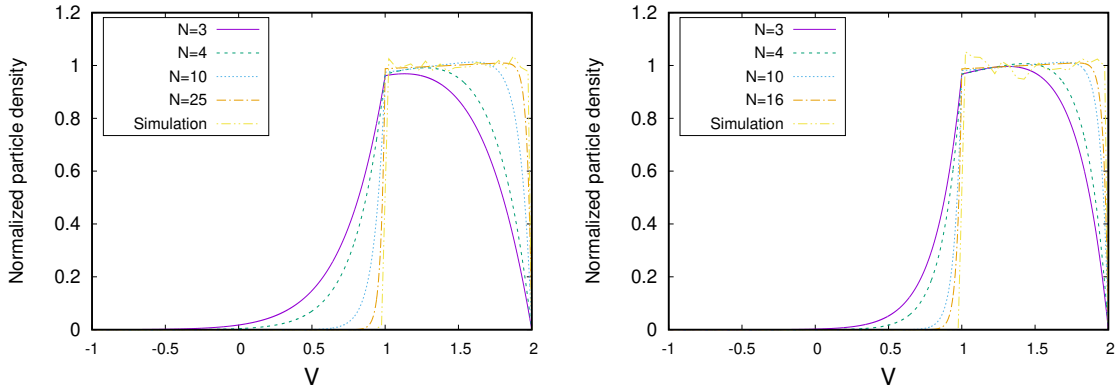


Figure 1: **Comparison of “plateau” distributions with profiles (1.7).** Graphs taken from [37]. *Left: $b = 1.5$. Right: $b = 2.2$.*

This behaviour suggests that we may think of the pseudo-equilibria sequence as a tool to analyse the asymptotic behaviour of the system when a large synaptic delay is taken into account. The aims of this work are twofold:

1. to analyse the sequence of pseudo-equilibria determined by the associated discrete system, and
2. to establish a connection between the long-term behaviour of the pseudo-equilibria sequence and the solutions of the nonlinear system (1.2).

Organisation of the paper. In Section 2 we define and analyse the firing rate and the pseudo-equilibria sequences. In Section 3 we prove the exponential convergence to equilibrium for the nonlinear system (1.2) for small connectivity parameter b and large delay d , by “following” the sequence of pseudo-equilibria, under some technical assumptions on the linear systems. A similar result was previously established through the use of the entropy method, and we present here different strategy which considers the relative entropy to the sequence of pseudo-equilibria. This approach looks promising to study a broader range of phenomena (such as periodic solutions or the approach of the plateau state), and served as a catalyst for the main ideas in our paper [43], where we prove local convergence results depending on the values of the transmission delay and the connectivity parameter. In Section 4 we provide the numerical evidence to support the connection between the sequence of pseudo-equilibria studied in Section 2 with the nonlinear system. This numerical work also suggests several conjectures on the possible extension of the results of Section 3 to cases with an arbitrary value of the parameter b . Section 5 is devoted to conclusions, discussion and possible extensions of our work. We also include an appendix with some of the technical results needed to prove Theorem 2.5.

2 Firing rate and pseudo-equilibria sequences

This section deals with the study of sequences of firing rates, $\{N_{k,\infty}\}_{k \geq 0}$, and pseudo-equilibria, $\{p_{k,\infty}\}_{k \geq 0}$. Let us first give their definition:

Definition 2.1 (Firing rate sequence). Given $b \in \mathbb{R}$, $V_R < V_F \in \mathbb{R}$, and I the function (1.6), the *firing rate sequence* $\{N_{k,\infty}\}_{k \geq 0}$ associated to an initial firing rate $N_{0,\infty} > 0$ is recursively defined by

$$N_{k+1,\infty} := \frac{1}{I(N_{k,\infty})} \quad k = 0, 1, 2, \dots \quad (2.1)$$

This sequence is well defined since $I(N) > 0$ for all $N > 0$. Associated to a firing rate sequence $\{N_{k,\infty}\}_{k \geq 0}$ we define the following pseudo-equilibria sequence:

Definition 2.2 (Pseudo-equilibria sequence). Given a firing rate sequence $\{N_{k,\infty}\}_{k \geq 0}$ its associated *pseudo-equilibria sequence* is the sequence

$$p_{k,\infty}(v) = N_{k,\infty} e^{-\frac{(v-bN_{k-1,\infty})^2}{2}} \int_{\max(v, V_R)}^{V_F} e^{\frac{(w-bN_{k-1,\infty})^2}{2}} dw, \quad k = 1, 2, \dots \quad (2.2)$$

The behaviour of these sequences depends only on the values of the connectivity parameter b , the diffusion coefficient a (which we consider to be 1), the reset potential V_R and the threshold potential V_F . Their definition is completely detached from the dynamics of the nonlinear system (1.2).

In the following theorems we show the monotonicity of the firing rate sequence $\{N_{k,\infty}\}_{k \geq 0}$, in terms of the number of solutions to the implicit equation

$$NI(N) = 1, \quad \text{with } 0 \leq N. \quad (2.3)$$

We have denoted the unknown in Equation (2.3) by N and hope that it will not cause any confusion with the firing rate of the nonlinear system (1.2). In this section we never consider the system (1.2), since we are only concerned with the behaviour of the firing rate sequence.

The number of solutions to Equation (2.3) was studied in [24]. Analytically it was shown that for $b < 0$ or for a small positive value of b there is only one solution, there is no solution if $b > 0$ is large, and there are at least two for intermediate positive values of b . The proof is based on the study of the monotone function $1/I(N)$ (increasing if $b > 0$ and decreasing if $b < 0$). However, rigorously proving the exact number of solutions in the excitatory case ($b > 0$) is not easy, due to the complexity of I . Numerically we observe that for positive b there are a maximum of two solutions, and at the value of b where the equation switches from having two solutions to none the function $1/I(N)$ has slope equal to 1 and positive second derivative (see right plot of Figure 2). These are the scenarios we consider in the following theorem for the case $b > 0$:

Theorem 2.3 (Monotonicity of the firing rate sequence $\{N_{k,\infty}\}_{k \geq 0}$ for excitatory networks). *Let us consider $0 < b$ and a firing rate sequence $\{N_{k,\infty}\}_{k \geq 0}$ (as given by Definition 2.1).*

1. *If Equation (2.3) has a unique solution N^* then:*

(a) If $N \mapsto 1/I(N)$ crosses the diagonal $N \mapsto N$ (in the sense that $N < 1/I(N)$ for $N < N^*$ and $1/I(N) < N$ for $N^* < N$), then:

- For $N_{0,\infty} \geq N^*$, the sequence $\{N_{k,\infty}\}_{k \geq 0}$ is decreasing and tends to N^* .
- For $N_{0,\infty} \leq N^*$, the sequence $\{N_{k,\infty}\}_{k \geq 0}$ is increasing and tends to N^* .

(b) If $N \mapsto 1/I(N)$ stays on one side of the diagonal $N \mapsto N$ (in the sense that $N < 1/I(N)$ for all $N \neq N^*$), then:

- For $N_{0,\infty} > N^*$, the sequence $\{N_{k,\infty}\}_{k \geq 0}$ diverges.
- For $N_{0,\infty} \leq N^*$, the sequence $\{N_{k,\infty}\}_{k \geq 0}$ is increasing and tends to N^* .

2. If Equation (2.3) has no solutions, then $\{N_{k,\infty}\}_{k \geq 0}$ diverges.

3. If Equation (2.3) crosses the diagonal $N \mapsto N$ at exactly two points $N_1^* < N_2^*$ (in the sense that $1/I(N) > N$ for $N < N_1^*$, $1/I(N) < N$ for $N_1^* < N < N_2^*$, and $1/I(N) > N$ for $N > N_2^*$) then:

- If $N_{0,\infty} \leq N_1^*$ then $\{N_{k,\infty}\}_{k \geq 0}$ is an increasing sequence which tends to N_1^* .
- If $N_1^* \leq N_{0,\infty} \leq N_2^*$ then $\{N_{k,\infty}\}_{k \geq 0}$ is a decreasing sequence which tends to N_1^* .
- If $N_2^* < N_{0,\infty}$ then $\{N_{k,\infty}\}_{k \geq 0}$ diverges.

Proof. The function I (see (1.6)) is a $C^\infty(0, \infty)$ function, which was studied in the proof of [24, Theorem 3.1], and can be rewritten as $I(N) = \int_0^\infty e^{-s^2/2} e^{-sbN} \frac{e^{sV_F} - e^{sV_R}}{s} ds$. Its k -th order derivative is

$$I^{(k)}(N) = (-b)^k \int_0^\infty s^{k-1} e^{-s^2/2} e^{-sbN} (e^{sV_F} - e^{sV_R}) ds, \quad (2.4)$$

and for b positive:

- $\frac{1}{I(N)}$ is an increasing function.
- $\frac{1}{I(0)} < \infty$.
- $\lim_{N \rightarrow \infty} \frac{1}{I(N)} = \infty$.

The firing rate sequence is a solution to the recursive equation

$$N_{k+1,\infty} = f(N_{k,\infty}), \quad f: \mathbb{R}_0^+ \rightarrow \mathbb{R}^+, \quad f(x) := \frac{1}{I(x)}, \quad (2.5)$$

where $\mathbb{R}^+ := \{x \in \mathbb{R} \mid x > 0\}$, $\mathbb{R}_0^+ := \{x \in \mathbb{R} \mid x \geq 0\}$, and we have seen that f is an increasing function. The behaviour of this type of discrete system is well known: its solutions are monotonic, and either diverge or converge to an equilibrium of the system. With the hypotheses of the theorem we have the following possibilities, since $f(0) > 0$:

- In case 1(a),
 - $N < f(N)$ for $N < N^*$.
 - $f(N) < N$ for $N^* < N$.

- In case 1(b), $N < f(N)$ for $N \neq N^*$.
- In case 2 we have $N < f(N)$ for all $N \geq 0$, since $0 < f(0)$.
- In case 3,
 - $N < f(N)$ for $N \in [0, N_1^*) \cup (N_2^*, +\infty)$.
 - $f(N) < N$ for $N \in (N_1^*, N_2^*)$.
 - $N < f(N)$ for $N \in (N_2^*, +\infty)$.

In cases 1 and 3, this is just part of the hypotheses of the result; in case 2 this is a consequence of $f(0) > 0$, and the facts that f is continuous and (by assumption in case 2) does not touch the diagonal.

1. If the initial condition is taken in an interval in which $N < f(N)$ then the sequence is increasing, because $N_{k,\infty} < f(N_{k,\infty}) = N_{k+1,\infty}$.
2. If the initial condition is taken in an interval in which $f(N) < N$ then the sequence is decreasing, because $N_{k+1,\infty} = f(N_{k,\infty}) < N_{k,\infty}$.

Whenever the sequence is decreasing, it is bounded below by a constant solution of Equation (2.5) and therefore converges to it (because there are no more equilibria in that interval). If the sequence is increasing, it either converges to an equilibrium, if bounded, or diverges. \square

Remark 2.4. As a consequence of the convergence of the firing rate sequences, given in Theorem 2.3, it follows:

1. If N^* is the only solution to Equation (2.3), then:
 - (a) In case 1.(a) of Theorem 2.3, $\frac{d}{dN} \frac{1}{I(N)}|_{N^*} \leq 1$.
 - (b) In case 1.(b) of Theorem 2.3, $\frac{d}{dN} \frac{1}{I(N)}|_{N^*} = 1$.

This behaviour is shown in plot on the right of Figure 2 with $b = 0$ or $b = 0.5$ for the first case and $b = 2.1$ the second case.

2. If Equation (2.3) has two solutions: N_1^* and N_2^* ($N_1^* < N_2^*$), then:
 - $0 \leq \frac{d}{dN} \frac{1}{I(N)}|_{N_1^*} \leq 1$.
 - $1 \leq \frac{d}{dN} \frac{1}{I(N)}|_{N_2^*}$.

This behaviour is shown in the plot on the right of Figure 2 with $b = 1.5$.

We analyse the inhibitory case ($b < 0$) in the following theorem, where two different behaviours appear although in this case Equation (2.3) has only one solution.

Theorem 2.5 (Monotonicity of the firing rate sequence $\{N_{k,\infty}\}_{k \geq 0}$ for inhibitory networks). *Assume $b < 0$ and consider a firing rate sequence $\{N_{k,\infty}\}_{k \geq 0}$. Then there exists a value $b^* < 0$ of the connectivity parameter b such that:*

- *If $b^* < b < 0$, the unique solution N^* to Equation (2.3) is asymptotically stable regarding firing rate sequences.*

- If $b < b^*$, there exist two values N^-, N^+ , $0 \leq \min(N^-, N^+) < N^* < \max(N^-, N^+)$, such that the sequence $\{N_{k,\infty}\}_{k \geq 0}$ tends to the 2-cycle $\{N^-, N^+\}$.

Proof. Step 1: The sequence of firing rates is either convergent or asymptotically 2-periodic. The proof, as in Theorem 2.3, is based on the study of the recursive equation:

$$N_{k+1,\infty} = f(N_{k,\infty}), \quad f(x) := \frac{1}{I(x)}, \quad (2.6)$$

where the function I , defined in (1.6), is a $C^\infty(0, \infty)$ increasing function if $b < 0$ (see (2.4) with $k = 1$). Therefore, for the inhibitory case, $f : [0, +\infty) \rightarrow \left[0, \frac{1}{I(0)}\right]$ since the function $1/I$ is decreasing, and, with the possible exception of the initial datum, $N_{0,\infty}$, all the other terms in the sequence fall within the interval $\left[0, \frac{1}{I(0)}\right]$. Moreover, in this case, Equation (2.3) has a unique solution, N^* , because $1/I(N)$ is a decreasing continuous function which tends towards 0, and $0 < 1/I(0)$.

The behaviour of this type of discrete system is easy to study, because f is a decreasing function and the solutions are bounded; they tend to the unique equilibrium or towards a 2-cycle. The proof of this result is as follows: denote by N^* the equilibrium of (2.6), and assume that $N_{0,\infty} \neq N_{2,\infty}$ (otherwise, the solution would be exactly a 2 cycle, or constantly equal to N^* if $N_{0,\infty} = N_{2,\infty} = N^*$). Thus, using that f is a decreasing function and $F := f \circ f$ is increasing:

- If $N_{0,\infty} < N_{2,\infty}$, then $N_{3,\infty} = f(N_{2,\infty}) \leq f(N_{0,\infty}) = N_{1,\infty}$ and $N_{2,\infty} = F(N_{0,\infty}) \leq F(N_{2,\infty}) = N_{4,\infty}$. Therefore, by induction we prove that $\{N_{2k,\infty}\}_{k \geq 0}$ is an increasing sequence and $\{N_{2k+1,\infty}\}_{k \geq 0}$ is a decreasing sequence.
- If $N_{0,\infty} > N_{2,\infty}$, then $N_{3,\infty} = f(N_{2,\infty}) \geq N_{1,\infty} = f(N_{0,\infty})$ and $N_{2,\infty} = F(N_{0,\infty}) \geq F(N_{2,\infty}) = N_{4,\infty}$. Therefore, by induction we prove that $\{N_{2k,\infty}\}_{k \geq 0}$ is a decreasing sequence and $\{N_{2k+1,\infty}\}_{k \geq 0}$ is an increasing sequence.

Moreover:

- If $N_{0,\infty} \leq N^*$, then $N^* = f(N^*) \leq f(N_{0,\infty}) = N_{1,\infty}$ and $N_{2,\infty} = f(N_{1,\infty}) \leq f(N^*) = N^*$. Therefore, by induction we prove that $0 \leq N_{2k,\infty} \leq N^* \leq N_{2k+1,\infty} \leq \frac{1}{I(0)}$ for $k = 0, 1, 2, \dots$
- If $N^* \leq N_{0,\infty}$, then $f(N_{0,\infty}) = N_{1,\infty} \leq N^* = f(N^*)$ and $f(N^*) = N^* \leq N_{2,\infty} = f(N_{1,\infty})$. Therefore, by induction we prove that $0 \leq N_{2k+1,\infty} \leq N^* \leq N_{2k,\infty} \leq \frac{1}{I(0)}$ for $k = 0, 1, 2, \dots$

So that in either case, both sequences, $\{N_{2k,\infty}\}_{k \geq 0}$ and $\{N_{2k+1,\infty}\}_{k \geq 0}$, are monotonic and bounded, hence convergent. Thus, considering

$$N^- := \lim_{k \rightarrow \infty} N_{2k+1,\infty} \text{ and } N^+ := \lim_{k \rightarrow \infty} N_{2k,\infty},$$

we obtain, since f is a continuous function, that $f(N^+) = N^-$ and there are two possibilities:

1. $N^- = N^+ = N^*$, so that the system tends towards the equilibrium.

2. $N^- \neq N^+$, so that the system tends towards the 2-cycle $\{N^-, N^+\}$, where $\min(N^-, N^+) < N^* < \max(N^-, N^+)$.

Step 2: Determination of b_* . The remainder of the proof concentrates on determining b^* , which must be the largest value at which N^* is asymptotically stable for our discrete iteration. When we need to emphasize the dependence of I on b we will use the notation $I(b, N)$ (and $f(b, N) := 1/I(b, N)$). We note that I is a decreasing function of b , since

$$\partial_b I(b, N) = -N \int_0^\infty e^{-s^2/2} e^{-sbN} (e^{sV_F} - e^{sV_R}) \, ds,$$

and consequently $1/I$ is increasing as a function of b (see Figure 2). Therefore, if $b_1 < b_2 < 0$, then $\frac{1}{I(b_1, N)} < \frac{1}{I(b_2, N)}$ and the solution to Equation (2.3) for $b = b_1$, is less than the solution for $b = b_2$, that is, $N_{b_1}^* < N_{b_2}^*$, with N_b^* denoting the (unique) solution to (2.3) for a given $b \leq 0$. Alternatively, one can prove that N_b^* is increasing in b by deriving implicitly in the equation $N_b^* I(b, N_b^*) = 1$ and observing that the derivative is positive, as follows:

$$\frac{dN_b^*}{db} = \frac{-N_b^* \partial_b I(b, N_b^*)}{I(b, N_b^*) + N_b^* \partial_N I(b, N_b^*)} \geq 0.$$

Consequently, N_b^* is an increasing function bounded from below by 0, so it has a limit when b tends to $-\infty$. On the other hand, $\bar{f}(N) := \lim_{b \rightarrow -\infty} f(b, N)$ loses continuity at $N = 0$, because $\bar{f}(0) > 0$, while it vanishes for $0 < N < \bar{f}(0)$. Therefore,

$$\bar{N}^* := \lim_{b \rightarrow -\infty} N_b^* = 0.$$

This is because if the limit was positive, $\bar{N}^* > 0$, then using the explicit expression of I we get $\lim_{b \rightarrow -\infty} f(b, N_b^*) = 0$, and therefore

$$0 = \lim_{b \rightarrow -\infty} f(b, N_b^*) = \lim_{b \rightarrow -\infty} N_b^* = \bar{N}^* > 0,$$

which is a contradiction.

(This was also proven in [32, Lemma 2.2]). Thus, in a certain sense, the system “loses” its equilibrium when b tends to $-\infty$, due to the loss of continuity of the function $1/I$ in the limit.

To determine whether or not the equilibrium of Equation (2.6), N_b^* , is asymptotically stable, we check whether $|f'(N_b^*)|$ is less than or greater than 1. With this aim, we define

$$g(b) := f'(N_b^*) = \frac{d}{dN} \frac{1}{I(N)} \Big|_{N_b^*} = \frac{-\partial_N I(b, N_b^*)}{I(b, N_b^*)^2} = -N_b^{*2} \partial_N I(b, N_b^*),$$

which is a continuous increasing function in $(-\infty, 0]$, due to the positivity of $g'(b)$, as proved in Lemma A.1. We note that $\lim_{b \rightarrow -\infty} g(b) = -\infty$ and $g(0) = f'(N_0^*) = 0$, thus there exists b^* such that $g(b^*) = -1$. Then, if $b < b^*$, thus $g(b) < -1$, which means that N_b^* is unstable for the discrete iteration, while for $b > b^*$, $g(b) > -1$ and N_b^* is stable. And as we proved above, if the equilibrium is unstable, the system tends to a 2-cycle. \square

Remark 2.6. We do not know how to prove analytically some further details in Theorem 2.5, due to the difficulty of working with the function I : the global stability of the equilibrium in the case $b^* \leq b < 0$, and the uniqueness of the two cycles, in the case $b < b^*$. However, we can check both numerically. Figure 3 shows the function $F(N) = f \circ f(N)$, for cases with $b < b^*$. F has only 3 fixed points, i.e., the equilibrium N^* and cycle $\{N^-, N^+\}$ corresponding to each value of b . Moreover, the 2-cycles appear as a bifurcation of the equilibrium, which is asymptotically stable for $b = b^*$, as this value is the starting point for the formation of 2-cycles. We also note that the 2-cycle $\{N^-, N^+\}$ becomes $\left\{0, \frac{1}{I(0)}\right\}$, approximately $\{0, 0.12\}$, when b tends to $-\infty$, as N_b^* tends to 0. For $b > b^*$ we observe an unique fixed point for $F(N)$, corresponding with the equilibrium N^* , so it is globally stable.

Remark 2.7. As a consequence of the convergence of the firing rate sequences, given in Theorem 2.5, it follows:

1. If $b_* < b < 0$, then $-1 \leq \frac{d}{dN} \frac{1}{I(N)}|_{N^*} < 0$, for N^* the only solution to Equation (2.3).
2. If $b < b_*$, then $\frac{d}{dN} \frac{1}{I(N)}|_{N^*} \leq -1$, for N^* the only solution to Equation (2.3).

We have numerically estimated $b^* \approx -9.4$ (see Figure 3). The plot on the left of Figure 2 shows the function $\frac{1}{I(N)}$ for $b < -9.4$ and for $b > -9.4$, where we can observe its slope at N^* .

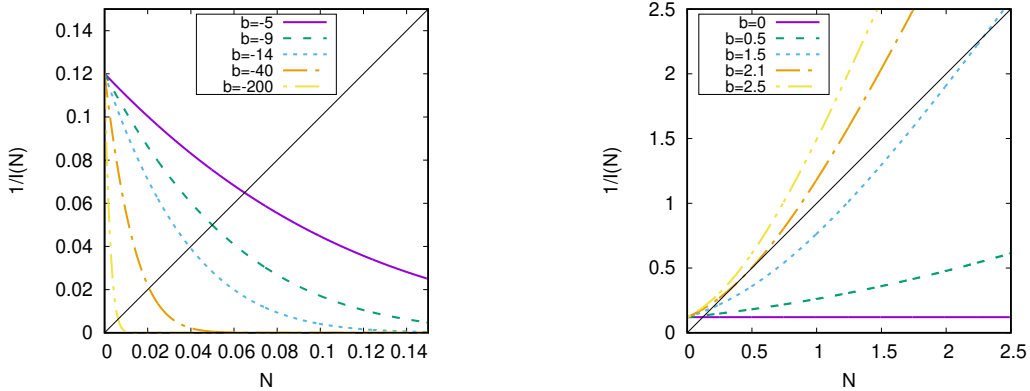


Figure 2: **Function $\frac{1}{I(N)}$ (see (1.6)) for different values of the connectivity parameter b .**

We recall that the number of solutions to the Equation (2.3) gives us the number of steady states of the nonlinear system (1.2). This number depends on the value of b (see [24]). For the excitatory case ($b > 0$) there is only one steady state if $b \leq V_F - V_R$. If $V_F - V_R < b$ there are two possibilities: there are at least two steady states (numerically no more than two steady states have been observed), or, if b is large enough, there is not steady states. The case $b = V_F - V_R$ is very interesting because this is the limit value for which the notion of physical solutions makes sense. Numerically this case was analysed in [37] and without delay ($d = 0$) the particle system evolves to a plateau distribution, if the initial condition is concentrated enough around V_F . In a limit sense, this plateau

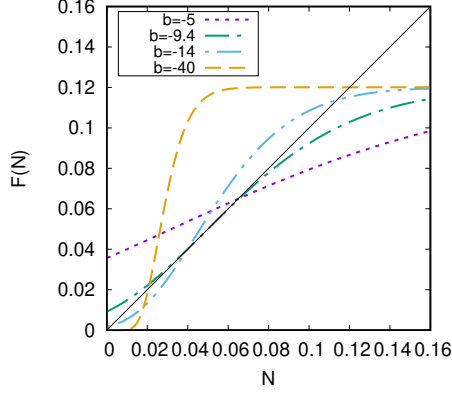


Figure 3: **Function $F := f \circ f$ with $f(N) = 1/I(N)$ (see (1.6)) for different (negative) values of the connectivity parameter b .**

profile is a stationary state of the system for $b = V_F - V_R$. However, the system tends to the unique steady state with bounded firing rate, if a large transmission delay is considered. For the inhibitory case ($b < 0$) there is only one steady state. Therefore, Theorems 2.3 and 2.5 can also be read in terms of the number of the steady states of the nonlinear system (1.2).

Remark 2.8. Theorem 2.3 does not include the case with more than two equilibria, which can be easily extended following the same strategy. For instance, if Equation (2.3) has three solutions (i.e. the nonlinear system (1.2) has three steady states), $N_1^* < N_2^* < N_3^*$, the sequence $\{N_{k,\infty}\}_{k \geq 0}$ tends to N_1^* , if $N_{0,\infty} \in (0, N_2^*)$, and to N_3^* , if $N_{0,\infty} \in (N_2^*, +\infty)$. In general, the behaviour of the sequence $\{N_{k,\infty}\}_{k \geq 0}$ depends on whether $N_k I(N_k) < 1$ or $1 < N_k I(N_k)$. In the first case the sequence is increasing, while in the second case the sequence is decreasing. When the sequence is decreasing it converges to some solution to Equation (2.3), while if the sequence is increasing it converges or diverges depending on whether it is bounded by a solution to the implicit equation or not.

The following theorem shows that the pseudo-equilibria sequence $\{p_{k,\infty}(v)\}_{k \geq 0}$ described in (2.2) tends to a stationary solution p_∞ of the nonlinear system (1.2) if its related sequence $\{N_{k,\infty}\}_{k \geq 0}$ (see (2.1)) converges to a finite value N_∞ , which is the firing rate of p_∞ .

Theorem 2.9. *Consider any nonnegative sequence $\{N_{k,\infty}\}_{k \geq 0}$, and its related pseudo-equilibria sequence $\{p_{k,\infty}(v)\}_{k \geq 0}$ described in (2.2). Assume $\lim_{k \rightarrow \infty} N_{k,\infty} = N_\infty < +\infty$. Then there exists $k_0 \in \mathbb{N}$ such that for all $k \geq k_0$ and all $N \in \mathbb{R}$ the following inequalities hold:*

$$\|p_{k+1,\infty}(v) - p_{k,\infty}(v)\|_\infty \leq C_{N_\infty} |N_{k,\infty} - N_{k-1,\infty}|, \quad (2.7)$$

$$\|\partial_v p_{k+1,\infty}(v) - \partial_v p_{k,\infty}(v)\|_\infty \leq C_{N_\infty} |N_{k,\infty} - N_{k-1,\infty}|, \quad (2.8)$$

$$\|p_{k+1,\infty}(v) - p_{k,\infty}(v)\|_{L^2(\varphi_N)} \leq C_{N_\infty} |N_{k,\infty} - N_{k-1,\infty}|, \quad (2.9)$$

$$\|\partial_v p_{k+1,\infty}(v) - \partial_v p_{k,\infty}(v)\|_{L^2(\varphi_N)} \leq C_{N_\infty} |N_{k,\infty} - N_{k-1,\infty}|, \quad (2.10)$$

where $C_{N_\infty} > 0$ is a constant that depends only on N_∞ , b , V_R and V_F , and also on N

in the case of (2.9)–(2.10). Similarly, for all $k \geq k_0$ and all $N \in \mathbb{R}$,

$$\|p_{k,\infty}(v) - p_\infty(v)\|_\infty \leq C_{N_\infty} |N_{k-1,\infty} - N_\infty|, \quad (2.11)$$

$$\|\partial_v p_{k,\infty}(v) - \partial_v p_\infty(v)\|_\infty \leq C_{N_\infty} |N_{k-1,\infty} - N_\infty|, \quad (2.12)$$

$$\|p_{k,\infty}(v) - p_\infty(v)\|_{L^2(\varphi_N)} \leq C_{N_\infty} |N_{k-1,\infty} - N_\infty|, \quad (2.13)$$

$$\|\partial_v p_{k,\infty}(v) - \partial_v p_\infty(v)\|_{L^2(\varphi_N)} \leq C_{N_\infty} |N_{k-1,\infty} - N_\infty|, \quad (2.14)$$

with $p_\infty = p_\infty(v)$ the steady state of the nonlinear system (1.2) with firing rate N_∞ .

Remark 2.10. In other words, this result states that pseudo-equilibrium $p_{k,\infty}$ given in (2.2), associated to a number N_{k-1} , depends continuously on N_{k-1} in a wide variety of norms including the Sobolev $W^{1,\infty}$ norm and weighted L^2 and H^2 norms. We have chosen to state it for a sequence, since it is the exact result which will be later used in Section 3.

Proof. We recall the expression of the pseudo-equilibrium

$$p_{k,\infty}(v) = N_{k,\infty} e^{-\frac{(v-bN_{k-1,\infty})^2}{2}} \int_{\max(v, V_R)}^{V_F} e^{\frac{(w-bN_{k-1,\infty})^2}{2}} dw,$$

where $N_{k,\infty} = I(N_{k-1,\infty})^{-1}$ and $I(N) = \int_{-\infty}^{V_F} e^{-\frac{(v-bN)^2}{2}} \int_{\max(v, V_R)}^{V_F} e^{\frac{(w-bN)^2}{2}} dw dv$. We define

$$g(v, N) := e^{-\frac{(v-bN)^2}{2}} \int_{\max(v, V_R)}^{V_F} e^{\frac{(w-bN)^2}{2}} dw, \quad h(v, N) := \frac{g(v, N)}{I(N)},$$

so that $h(v, N_{k-1,\infty}) = p_{k,\infty}(v)$ and $h(v, N_\infty) = p_\infty(v)$ (since it must hold $1 = N_\infty I(N_\infty)$). Through a first-order Taylor expansion in N we can write the difference between two consecutive elements of the sequence $\{p_{k,\infty}\}_{k \geq 0}$ as

$$p_{k+1,\infty}(v) - p_{k,\infty}(v) = \partial_N h(v, \xi_k) (N_{k,\infty} - N_{k-1,\infty}),$$

where ξ_k is a value located between $N_{k-1,\infty}$ and $N_{k,\infty}$. Due to the convergence of the sequence $N_{k,\infty}$, there exists $k_0 \in \mathbb{N}$ such that $N_{k-1,\infty}$ and $N_{k,\infty} \in (N_\infty/2, 2N_\infty)$ for all $k \geq k_0$. In particular, $\xi_k \in (N_\infty/2, 2N_\infty)$ for all $k \geq k_0$. Therefore, it is enough to show that

$$|\partial_N h(v, N)| < C_{N_\infty}, \quad (2.15)$$

uniformly in $v \in (-\infty, V_F]$ and $N \in (N_\infty/2, 2N_\infty)$, with some constant C_{N_∞} which depends only on N_∞, b, V_R and V_F . This would prove inequality (2.7).

By computing $\partial_N h(v, N)$ we obtain

$$\partial_N h(v, N) = \frac{\partial_N g(v, N)}{I(N)} - \frac{I'(N)}{I(N)^2} g(v, N). \quad (2.16)$$

In order to show (2.15) it is enough to study each term: from the expression of $g(v, N)$ one sees that it is bounded as needed, since $e^{-\frac{(v-bN)^2}{2}}$ and $ve^{-\frac{(v-bN)^2}{2}}$ are uniformly bounded in $v \in (-\infty, V_F]$ and $N \in (N_\infty/2, 2N_\infty)$; $I(N)$ is uniformly bounded below

for $N \in (N_\infty/2, 2N_\infty)$, and $|I'(N)|$ (which can be explicitly written) is bounded above in the same interval. Finally, one can explicitly write $\partial_N g(v, N)$,

$$\partial_N g(v, N) = b(v - bN)g(v, N) - be^{-\frac{(v-bN)^2}{2}} \left(e^{\frac{(V_F-bN)^2}{2}} - e^{\frac{(\max(v, V_R)-bN)^2}{2}} \right),$$

and show it is also uniformly bounded in the needed range of v and N . This shows (2.7). With a completely analogous calculation we prove (2.11), since

$$p_{k,\infty}(v) - p_\infty(v) = \partial_N h(v, \xi_k) (N_{k-1,\infty} - N_\infty),$$

for some ξ_k between $N_{k-1,\infty}$ and N_∞ . By checking that $\|\partial_N h(\cdot, M)\|_{L^2(\varphi_N)}$ is bounded uniformly for $M \in (N_\infty/2, 2N_\infty)$ we also prove (2.9), and very similarly (2.13).

For the derivatives with respect to v we write

$$\partial_v p_{k,\infty}(v) = \frac{1}{I(N_{k-1,\infty})} \partial_v g(v, N_{k-1,\infty}) =: \tilde{h}(v, N_{k-1,\infty})$$

and

$$\partial_v p_{k+1,\infty}(v) - \partial_v p_{k,\infty}(v) = \partial_N \tilde{h}(v, \xi_k) (N_{k,\infty} - N_{k-1,\infty}).$$

A similar analysis of $\partial_N \tilde{h}(v, N)$ proves the remaining points (2.8), (2.10), (2.12) and (2.14). \square

In the inhibitory case, the firing rate sequence may converge to a 2-cycle (see Theorem 2.5). We show the long-term behaviour of the pseudo-equilibria sequences in those cases in the following theorem.

Theorem 2.11. *Let us consider the firing rate sequence $\{N_{k,\infty}\}_{k \geq 0}$ given in (2.1), and its related pseudo-equilibria sequence $\{p_{k,\infty}(v)\}_{k \geq 0}$ described in (2.2). Assume the pseudo-equilibria sequence $\{N_{k,\infty}\}_{k \geq 0}$ tends to the 2-cycle $\{N^-, N^+\}$. Then there exists $k_0 \in \mathbb{N}$ such that for all $k \geq k_0$ the following inequalities hold:*

$$\|p_{2k,\infty}(v) - p_{2k-2,\infty}(v)\|_\infty \leq C_{N^-} |N_{2k-1,\infty} - N_{2k-3,\infty}|, \quad (2.17)$$

$$\|p_{2k+1,\infty}(v) - p_{2k-1,\infty}(v)\|_\infty \leq C_{N^+} |N_{2k,\infty} - N_{2k-2,\infty}|, \quad (2.18)$$

where $C_{N^-}, C_{N^+} > 0$ depend on N^- and N^+ , respectively, and b, V_F and V_R . Similarly, for all $k \geq k_0$

$$\|p_{2k,\infty}(v) - p^-(v)\|_\infty \leq C_{N^-} |N_{2k-1,\infty} - N^-|,$$

$$\|p_{2k+1,\infty}(v) - p^+(v)\|_\infty \leq C_{N^+} |N_{2k,\infty} - N^+|,$$

where $p^-(v), p^+(v)$ are pseudo-equilibria of the nonlinear system (1.2) (see (1.7)), with p^- associated to N^+ and p^+ associated to N^- .

Proof. This is a direct consequence of Theorem 2.9, by considering the sequences $\{N_{2k-1,\infty}\}_{k \geq 1}$ and $\{N_{2k,\infty}\}_{k \geq 0}$, which converge to N^- and N^+ , respectively. The associated pseudo-equilibria sequences are then $\{p_{2k,\infty}\}$ and $\{p_{2k+1,\infty}\}$, respectively, and the statement is a consequence of Theorem 2.9 applied to them. \square

We point out that the behaviour of the pseudo-equilibria sequence is determined by the limit of the firing rate sequence, in case it exists, for all $b \in \mathbb{R}$. And there is a relation between the nonlinear system (1.2) and that long-term behaviour:

- In the excitatory case ($b > 0$) the pseudo-equilibria sequence $\{p_{k,\infty}(v)\}_{k \geq 0}$:
 - converges to the unique steady state of the nonlinear system (1.2), if b is small.
 - converges to the steady state with lower firing rate of the nonlinear system (1.2), if the system has two stationary solutions and if $\{N_{k,\infty}\}_{k \geq 0}$ has finite limit.
- In the inhibitory case ($b < 0$) the pseudo-equilibria sequence $\{p_{k,\infty}(v)\}_{k \geq 0}$ tends to the unique stationary solution $p_\infty(v)$ of the nonlinear system (1.2), if $b^* < b$. Otherwise, if $b < b^*$, it tends to a 2-cycle $\{p^-(v), p^+(v)\}$, which are pseudo-equilibria of the nonlinear system (1.2).

To prove the convergence of the pseudo-equilibria sequence we use the fact that the limit of $\{N_{k,\infty}\}_{k \geq 0}$ is finite or is a 2-cycle, so it could not be used in case the sequence diverges. However, in that case, it could be prove that the sequence of pseudo-equilibria $\{p_{k,\infty}(v)\}_{k \geq 0}$ tends to plateau distribution (point-wise in $(-\infty, V_R) \cup (V_R, V_F)$).

In the following section we use Theorem 2.9 to prove the convergence to equilibrium of solutions to the nonlinear system (1.2) in the weakly connected case, by following the associated pseudo-equilibria sequence. As presented, this technique only works in weakly connected networks, but it might be possible to use it for a wider range of b .

3 Convergence to equilibrium along the pseudo equilibria sequence for weakly connected networks

In this section we study the long-term behaviour of the nonlinear system (1.2), considering large transmission delay values, by following the pseudo-equilibria (2.2) for weakly connected networks. To do this, we consider the solution to the Cauchy problem associated with (1.2) (remember we assume $a = 1$):

$$\begin{cases} \partial_t p(v, t) + \partial_v [(-v + bN(t-d)) p(v, t)] - \partial_v^2 p(v, t) = \delta(v - V_R) N(t), \\ N(t) = -\partial_v p(V_F, t), \text{ for } t \geq 0, \\ p(0, v) = p_0(v), \text{ and, } N(t) = -\partial_v p_0(V_F) \quad t \in [-d, 0], \end{cases} \quad (3.1)$$

We view this solution as a sequence of functions, considering time intervals of length d . Our initial condition is always a constant on $[-d, 0]$, and we observe that the system becomes linear for $0 \leq t < d$, since $N(t-d)$ is constant. Therefore, for $0 \leq t < d$, the Cauchy problem (3.1) behaves like a linear problem of the form

$$\begin{cases} \partial_t p(v, t) + \partial_v [(-v + b\bar{N}) p(v, t)] - \partial_v^2 p(v, t) = \delta(v - V_R) N(t), \\ N(t) = -\partial_v p(V_F, t), \quad t \geq 0, \\ p(0, v) = p_0(v), \text{ with } \bar{N} = -\partial_v p_0(V_F) \geq 0. \end{cases} \quad (3.2)$$

During that interval of time, $[0, d)$, we obtain $N(t)$, which appears in the drift term of the following period of time with size d , $[d, 2d)$. Proceeding in the same way for the

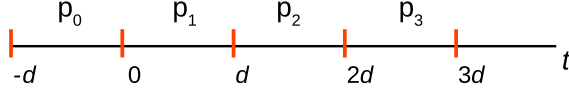


Figure 4: **Schematic representation of the solution to the Cauchy problem (3.1) in time through the sequence $p_k(v, t)$ given by (3.3).**

following time intervals $[kd, (k+1)d]$ with $k = 2, 3, \dots$, the nonlinear problem (3.1) is equivalent to a sequence of linear problems of the type

$$\begin{cases} \partial_t p(v, t) + \partial_v [h(v, \bar{N}(t)) p(v, t)] - \partial_v^2 p(v, t) = \delta(v - V_R) N(t), \\ N(t) = -\partial_v p(V_F, t), \quad t \geq 0, \end{cases}$$

where $\bar{N}(t)$ is a known function. To better describe the idea consider the following notation (see Figure 4):

$$p_{k+1}(v, t) := p(v, t + kd), \quad \text{with } t \in [0, d], \quad v \in (-\infty, V_F] \text{ and } k = 0, 1, 2, \dots \quad (3.3)$$

In other words, $p_{k+1}(v, t) \equiv p(v, \bar{t})$, with $\bar{t} := t + kd \in [kd, (k+1)d]$. Similarly,

$$N_k(t) := N(t + kd), \quad t \in [-d, 0], \quad k = 0, 1, 2, \dots$$

Hence we write the nonlinear problem (3.1) in any interval $(kd, (k+1)d)$, as follows: for $t \in (0, d)$ and $k = 1, 2, \dots$

$$\begin{cases} \partial_t p_k(v, t) + \partial_v [(-v + bN_{k-1}(t-d)) p_k(v, t)] - \partial_v^2 p_k(v, t) = \delta(v - V_R) N_k(t), \\ N_k(t) = -\partial_v p_k(V_F, t), \quad p_k(V_F) = 0, \end{cases} \quad (3.4)$$

Its related stationary problem is given by

$$\begin{cases} \partial_v [(-v + bN_{k-1, \infty}) p_{k, \infty}(v)] - \partial_v^2 p_{k, \infty}(v) = \delta(v - V_R) N_{k, \infty}, \\ N_{k, \infty} = -\partial_v p_{k, \infty}(V_F), \quad \text{and } \int_{-\infty}^{V_F} p_{k, \infty}(v) dv = 1, \end{cases} \quad (3.5)$$

whose unique solution is the pseudo-equilibria sequence (see (2.2))

$$p_{k, \infty}(v) = N_{k, \infty} e^{-\frac{(v - bN_{k-1, \infty})^2}{2}} \int_{\max(v, V_R)}^{V_F} e^{\frac{(w - bN_{k-1, \infty})^2}{2}} dw, \quad (3.6)$$

given in terms of the firing rate sequence (2.1), with $N_{0, \infty} := -\partial_v p_0(V_F)$.

Our purpose is to show that one may prove convergence to equilibrium of bounded solutions p to the nonlinear system by following the sequence of pseudo-equilibria $p_{k, \infty}$. For this we need to assume several properties of the linear system, which are reasonable in view of our recent results in [43]. In order to describe these assumptions we consider the space X given by

$$X := \{u \in \mathcal{C}(-\infty, V_F] \cap \mathcal{C}^1(-\infty, V_R] \cap \mathcal{C}^1[V_R, V_F] \mid u(V_F) = 0 \text{ and } \|u\|_X < \infty\}, \quad (3.7)$$

with

$$\|u\|_X := \|u\|_\infty + \|\partial_v u\|_\infty + \|u\|_{L^2(\varphi)} + \|\partial_v u\|_{L^2(\varphi)} \quad (3.8)$$

and

$$\varphi(v) := \exp\left(\frac{v^2}{2}\right), \quad v \in (-\infty, V_F].$$

This is the space of continuous functions on $(-\infty, V_F]$ which are \mathcal{C}^1 except possibly at $v = V_R$, where they must still have one-sided derivatives; and which are in the space H^1 with the Gaussian weight φ (so they are strongly decaying functions for $v \rightarrow -\infty$). The main merit of this space is that the firing rate $-\partial_v p(t, V_F)$ is a continuous operator in this norm. Our main assumptions on the associated linear equation are the following:

1. **(Spectral gap.)** The semigroup e^{tL} associated to the linear equation (3.2) has a spectral gap in the space X . That is, there exist constants $\lambda > 0$, $C \geq 1$ such that for all initial conditions $u_0 \in X$ with zero integral, it holds that

$$\|e^{tL}u_0\|_X \leq Ce^{-\lambda t}\|u_0\|_X \quad \text{for all } t \geq 0. \quad (3.9)$$

We assume this property holds uniformly for any \bar{N} close to an equilibrium firing rate N_∞ of the nonlinear equation (1.2).

2. **(Regularization property.)** There exist constants $\lambda > 0$, $\tilde{C} \geq 1$ such that for all initial conditions $u_0 \in L^2(\varphi)$ with zero integral, the following inequality holds:

$$\|e^{tL}u_0\|_X \leq \tilde{C}t^{-3/4}e^{-\lambda t}\|u_0\|_{L^2(\varphi)} \quad \text{for all } t > 0. \quad (3.10)$$

Again, we assume this property holds uniformly for any \bar{N} close to an equilibrium firing rate N_∞ of the nonlinear equation (1.2). We point out that the exponent $-3/4$ here is the same as for the standard Fokker-Planck equation

$$\partial_t p = \partial_v^2 p + \partial_v(vp).$$

Similar results to these assumptions are given in [43]. A proof of them can be given by using the techniques developed there, but this is not the aim of this paper and we defer a more detailed study of these spectral properties to a future work.

We will prove the following result:

Theorem 3.1. *Take $b \in \mathbb{R}$. Let us consider an initial condition $p_0 \in X$ for the nonlinear system (1.2) such that the firing rate sequence $\{N_{k,\infty}\}_{k \geq 0}$ with initial condition $N_{0,\infty} = -\partial_v p_0(V_F)$ converges to a certain value $N_\infty > 0$ (which must then satisfy $N_\infty I(N_\infty) = 1$). Let p_∞ be the stationary solution to (1.2) with firing rate N_∞ . Assume the spectral gap and regularisation properties stated before this theorem. Let $p = p(v, t)$ be the solution to (1.2) with initial data $p(v, t) = p_0(v)$ for all $v \in (-\infty, V_F]$ and all $t \in [-d, 0]$. Let us assume that there exists $K > 0$ such that*

$$\|p(\cdot, t)\|_X \leq K \quad \text{for all } t \geq 0. \quad (3.11)$$

Then there exist $d_0, b_0, Q, \mu > 0$ such that the solution p to the nonlinear system (1.2) with $d > d_0$, $|b| < b_0$, and initial condition p_0 satisfies

$$\|p(\cdot, t) - p_\infty(\cdot)\|_X \leq Qe^{-\mu t}\|p_0 - p_\infty\|_X \quad \text{for all } t \geq 0. \quad (3.12)$$

Remark 3.2. Assumption (3.11) in Theorem 3.1 merits an explanation. Our result only gives the behaviour of solutions which are *uniformly bounded in time* (which is consistent with convergence to equilibrium). It is known that solutions may blow up if the delay $d = 0$, and when $d > 0$ we do not know whether there may be solutions with diverging values of $N(t)$ as $t \rightarrow +\infty$. Our result applies only to solutions whose firing rate $N(t)$ is uniformly bounded for all times. Once we know the firing rate $N(t)$ is bounded it may be possible to carry out regularisation estimates to show that $\|p(t, \cdot)\|_X$ is uniformly bounded for all times, but we assume the latter stronger condition to avoid these technical details.

The proof of Theorem 3.1 is based on: 1) our spectral hypotheses on e^{tL} , 2) the uniform boundedness hypothesis on $\|p(t, \cdot)\|_X$ and 3) Theorem 2.9, which shows that

$$\|p_{k+1, \infty} - p_{k, \infty}\|_X \leq C_{N_\infty} |N_{k, \infty} - N_{k-1, \infty}|, \quad (3.13)$$

and, therefore $\|p_{k+1, \infty} - p_{k, \infty}\|_X \rightarrow 0$ as $\lim_{k \rightarrow \infty} N_{k, \infty} = N_\infty$. We will also need the following two elementary lemmas. The first one is a discrete version of the variation of constants technique, which can be checked in a straightforward way and we give without proof:

Lemma 3.3 (Discrete variation of constants). *Let M be a linear operator on a certain vector space E , and $\{b_k\}_{k \geq 0}$ any sequence in E . Then, given $a_0 \in E$, the sequence*

$$a_k := M^k a_0 + \sum_{i=0}^{k-1} M^{k-i-1} b_i, \quad k = 1, 2, \dots$$

is the (unique) solution to the linear equation

$$a_k = M a_{k-1} + b_{k-1}, \quad k = 1, 2, \dots \quad (3.14)$$

The second lemma needed for the proof of Theorem 3.1 is a discrete version of Gronwall's Lemma.

Lemma 3.4 (Discrete Gronwall's Lemma). *If ϕ_k is a positive sequence and $W \in \mathbb{R}$, $V \geq 0$ are constants such that $\phi_k \leq W + V \sum_{i=0}^{k-1} \phi_i$ for $k \geq 0$, then $\phi_k \leq W e^{kV}$ for all $k \geq 0$.*

Proof. To prove the result we define the sequence $\psi_k := W + V \sum_{i=0}^{k-1} \phi_i$ for $k \geq 1$ and $\psi_0 := W$. We compute the difference between two consecutive elements of that sequence and then we write it down in terms of the sequence ϕ_k :

$$\psi_k - \psi_{k-1} = V \phi_{k-1} \leq V \left(W + V \sum_{i=0}^{k-2} \phi_i \right) = V \psi_{k-1},$$

which leads to

$$\phi_{k-1} \leq \psi_{k-1},$$

and

$$\psi_k \leq (1 + V) \psi_{k-1} \implies \psi_k \leq (1 + V)^k \psi_0 = (1 + V)^k W.$$

Then we have the result, since $(1 + V) \leq e^V$:

$$\phi_k \leq (1 + V)^k W < W e^{kV}. \quad \square$$

Proof of Theorem 3.1. The proof is based on the study of the nonlinear system (1.2) in time intervals of size d , in which the system becomes linear. To do that we start with the nonlinear system (3.4) for $t \in (0, d)$ and $k = 1, 2, \dots$, and define

$$u_k(v, t) := p_k(v, t) - p_{k, \infty}(v),$$

the differences to the pseudo-equilibria $p_{k, \infty}(v)$. With this notation we rewrite the nonlinear system (3.4), splitting the equation in a linear part plus a nonlinear part:

$$\partial_t u_k(v, t) = L_{k-1} u_k(v, t) + b(N_{k-1, \infty} - N_{k-1}) \partial_v p_k(v, t),$$

with the same Dirichlet boundary condition as before and defining the linear operator L_{k-1} , associated to the firing rate $N_{k-1, \infty}$, acting on $u = u(v)$, by

$$L_{k-1} u := \partial_v(v - bN_{k-1, \infty} u) + \partial_v^2 u + \delta(v - V_R) N_u,$$

where $N_u := -\partial_v u(V_F)$ emphasises that N_u is the firing rate associated to u . By Duhamel's formula we get

$$u_k(v, t) = e^{tL_{k-1}} u_k(v, 0) + b \int_0^t (N_{k-1, \infty} - N_{k-1}(s)) e^{(t-s)L_{k-1}} \partial_v p_k(v, s) ds.$$

Taking the X norm we note that $|N_{k-1, \infty} - N_{k-1}(t)| \leq \|u_k(\cdot, t)\|_X$, and using the spectral gap of L_{k-1} in X :

$$\|e^{tL_{k-1}} u_0\|_X \leq C e^{-\lambda t} \|u_0\|_X, \quad 1 \leq C,$$

we have, for all $t \geq 0$:

$$\begin{aligned} \|u_k(\cdot, t)\|_X &\leq C e^{-\lambda t} \|u_k(\cdot, 0)\|_X + |b| \int_0^t |N_{k-1, \infty} - N_{k-1}(s)| \|e^{(t-s)L_{k-1}} \partial_v p_k(\cdot, s)\|_X ds \\ &\leq C e^{-\lambda t} \|u_k(\cdot, 0)\|_X + |b| \int_0^t \|u_{k-1}(\cdot, s)\|_X \|e^{(t-s)L_{k-1}} \partial_v p_k(\cdot, s)\|_X ds \\ &\leq C e^{-\lambda t} \|u_k(\cdot, 0)\|_X + \tilde{C} |b| \int_0^t e^{-\lambda(t-s)} (t-s)^{-3/4} \|u_{k-1}(\cdot, s)\|_X \|\partial_v p_k(\cdot, s)\|_{L^2(\varphi)} ds, \end{aligned}$$

where in the last inequality we used third hypothesis of the theorem, written in this particular case as

$$\|e^{(t-s)L_{k-1}} \partial_v p_k(\cdot, s)\|_X \leq \tilde{C} (t-s)^{-3/4} e^{-\lambda(t-s)} \|\partial_v p_k(\cdot, s)\|_{L^2(\varphi)}.$$

Remark 3.5. We are considering the same value of λ for all the spectral gaps of the operators L_k with $k = 1, 2, \dots$, because these values come from the Poincaré's like inequality used to prove the spectral gap of the linear equation in the space $L^2_{(p_{\infty}^{-1})}$ (see [24, Appendix]). These values depend only on the tails of the pseudo-equilibria $p_{k, \infty}$ and, considering that they convergence to p_{∞} (see Theorem 2.9), we may take a value λ valid for all k .

After this we can bound the $L^2(\varphi)$ norm of the derivative of p_k as

$$\|\partial_v p_k(\cdot, t)\|_{L^2(\varphi)} \leq \|\partial_v u_k(\cdot, t)\|_{L^2(\varphi)} + \|\partial_v p_{k, \infty}(\cdot)\|_{L^2(\varphi)} \leq \|u_k(\cdot, t)\|_X + \bar{C},$$

with $\bar{C} > 0$, and, using (3.11), and denoting the new constant again by K , we have $\|u_k(\cdot, s)\|_X \leq K < \infty \forall s \in [0, t] \subseteq [0, d]$. Thus, with the constant out of the integral and renaming it as $C_b := \bar{C}|b| (K + \bar{C})$, we get

$$\|u_k(\cdot, t)\|_X \leq C e^{-\lambda t} \|u_k(\cdot, 0)\|_X + C_b \int_0^t e^{-\lambda(t-s)} (t-s)^{-3/4} \|u_{k-1}(\cdot, s)\|_X ds. \quad (3.15)$$

Taking into account that $p_k(v, 0) = p_{k-1}(v, d)$, $u_{k-1}(v, d) := p_{k-1}(v, d) - p_{k-1, \infty}(v)$, and $u_k(v, 0) := p_k(v, 0) - p_{k, \infty}(v)$, we can write $u_k(v, 0) = u_{k-1}(v, d) + (p_{k-1, \infty}(v) - p_{k, \infty}(v))$, which, taking the X norm in v , leads to

$$\|u_k(\cdot, 0)\|_X \leq \|u_{k-1}(\cdot, d)\|_X + \delta_k$$

with $\delta_k := \|p_{k-1, \infty} - p_{k, \infty}\|_X$. By using the definitions $f_k(t) := e^{\lambda t} \|u_k(\cdot, t)\|_X$ and $\epsilon(t) := e^{-\lambda t}$, we rewrite the previous inequality as $f_k(0) \leq e^{-\lambda d} f_{k-1}(d) + \delta_k$, and (3.15) as

$$f_k(t) \leq C \epsilon(d) f_{k-1}(d) + C \delta_k + C_b \int_0^t f_{k-1}(s) (t-s)^{-3/4} ds, \quad (3.16)$$

which can be rewritten, in terms of the linear operators

$$A f_k(t) := C f_k(d), \quad B f_k := C_b \int_0^t f_k(s) (t-s)^{-3/4} ds \quad \text{and} \quad h f_{k-1} := \epsilon(d) A f_{k-1},$$

in the following way:

$$f_k \leq (\epsilon(d)A + B) f_{k-1} + C \delta_k = h_{k-1} + B f_{k-1} + C \delta_k, \quad (3.17)$$

To prove the decay of $\|u_k(\cdot, t)\|_X$ we shall proceed in two steps: first we study the solution to $f_k \leq h_{k-1} + B f_{k-1}$ and prove its convergence. Secondly we extend the converge to the complete sequence f_k , using that $\delta_k \rightarrow 0$ (see Theorem 2.9 and previous comments before the proof).

First step: Study of the recurrence $f_k \leq h_{k-1} + B f_{k-1}$.

We note that if f_k satisfies the inequality $f_k \leq h_{k-1} + B f_{k-1}$, then $f_k \leq x_k$, where x_k is the solution to the recursive equation $x_k = h_{k-1} + B x_{k-1}$ with initial condition $x_k = f_0$. Then, using the Lemma 3.3 to x_k we obtain

$$f_k \leq B^k f_0 + \sum_{i=0}^{k-1} B^{k-i-1} h_i.$$

Therefore we need to estimate $B^k f_0$ for $k = 1, 2, \dots$. After some computations we obtain

$$B^k(f_0) \leq \|f_0\|_\infty t^{\frac{k}{4}} \frac{(C_b \Gamma(\frac{1}{4}))^k}{\Gamma(1 + \frac{k}{4})}, \quad 0 < t < d,$$

by using

$$\int_0^t s^n (t-s)^{-3/4} ds = t^{n+\frac{1}{4}} \beta(n+1, \frac{1}{4}), \quad n = 1, 2, \dots$$

and properties of the Gamma, Γ , and Beta, β , functions, as

$$B^k(f_0) \leq (C_b)^k \|f_0\|_\infty t^{\frac{k}{4}} \prod_{i=0}^{k-1} \beta\left(1 + \frac{k}{4}, \frac{1}{4}\right) = (C_b)^k \|f_0\|_\infty t^{\frac{k}{4}} \prod_{i=0}^{k-1} \frac{\Gamma(1 + \frac{k}{4})\Gamma(\frac{1}{4})}{\Gamma(1 + \frac{k+1}{4})}.$$

Then we use the $\|\cdot\|_\infty$ norm in $t \in [0, d]$ so that the following inequality holds:

$$\|f_k\|_\infty \leq \frac{(d^{1/4}C_b\Gamma(\frac{1}{4}))^k}{\Gamma(1 + \frac{k}{4})} \|f_0\|_\infty + \sum_{i=0}^{k-1} \frac{(d^{1/4}C_b\Gamma(\frac{1}{4}))^{k-i-1}}{\Gamma(1 + \frac{k-i-1}{4})} \|h_i\|_\infty,$$

or, equivalently

$$\|f_k\|_\infty \leq \frac{(d^{1/4}C_b\Gamma(\frac{1}{4}))^k}{\Gamma(1 + \frac{k}{4})} \|f_0\|_\infty + C\epsilon(d) \sum_{i=0}^{k-1} \frac{(d^{1/4}C_b\Gamma(\frac{1}{4}))^{k-i-1}}{\Gamma(1 + \frac{k-i-1}{4})} \|f_i\|_\infty. \quad (3.18)$$

Bearing in mind that $C > 1$, we consider $C \frac{(d^{1/4}C_b\Gamma(1/4))^k}{\Gamma(1 + \frac{k}{4})} \leq \eta_{b,d} e^{-k}$ for an appropriate $\eta_{b,d}$, which can be computed by finding the maximum of the function

$$g(k) := \frac{(d^{1/4}C_b\epsilon\Gamma(1/4))^k}{\Gamma(1 + \frac{k}{4})} = \frac{M^k}{\Gamma(1 + \frac{k}{4})} \quad \text{with} \quad M := d^{1/4}C_b\epsilon\Gamma(1/4).$$

We take the logarithm of $g(k)$ and then we find a quantity that bounds the maximum of function $g(k)$ by approximating the gamma function using the Stirling's formula

$$\Gamma\left(1 + \frac{k}{4}\right) \geq \left(\frac{k}{4}\right)^{\frac{k}{4}} e^{-\frac{k}{4}},$$

such that

$$\log g(k) \leq k \log M + \frac{k}{4} - \frac{k}{4} \log \frac{k}{4} =: \hat{g}(k).$$

Studying the first derivative of function $\hat{g}(k)$ we compute the maximum, given by $\hat{g}(4M^4)$ and then bounding the function $g(k)$ as $g(k) \leq e^{M^4}$. This procedure allows us to define the quantity $\eta_{b,d}$ as

$$\eta_{b,d} := C e^{M^4} = C e^{d(|\tilde{C}(\bar{C}+K)\epsilon\Gamma(1/4)|)^4} = C e^{d|b|^4 \hat{C}},$$

having unified all constants in the exponential as $\hat{C} := \tilde{C}(\bar{C} + K)\epsilon\Gamma(1/4)$.

Now we can rewrite expression (3.18) through the following inequality:

$$\|f_k\|_\infty \leq \eta_{b,d} e^{-k} \|f_0\|_\infty + \eta_{b,d} \epsilon(d) \sum_{i=0}^{k-1} e^{-(k-i-1)} \|f_i\|_\infty.$$

Finally, if we define $\phi_k := e^k \|f_k\|_\infty$, $W := \eta_{b,d} \|f_0\|_\infty$ and $V := \eta_{b,d} \epsilon(d) e$, we can write the previous inequality as

$$\phi_k \leq W + V \sum_{i=0}^{k-1} \phi_i. \quad (3.19)$$

Now we use the discrete Gronwall's Lemma 3.4 to turn the equation (3.19) into the following $\phi_k \leq We^{kV}$, which leads to

$$\|f_k\|_\infty \leq We^{k(V-1)}. \quad (3.20)$$

Equation (3.20) implies that V must be less than 1 in order to obtain convergence to 0 of the sequence $\|u_k(t)\|_X$, so that the condition over the delay is the following:

$$d > \frac{1 + \log(\eta_{b,d})}{\lambda} = \frac{1 + \log C + \hat{C}db^4}{\lambda},$$

or, equivalently

$$d > \frac{1 + \log C}{\lambda - \hat{C}b^4}. \quad (3.21)$$

This inequality requires a smallness condition on b , since $\lambda - \hat{C}b^4$ needs to be positive. That is: we can take d satisfying (3.21), only if $|b|^4 < \lambda/\hat{C}$.

Second step: Study of $f_k \leq h_{k-1} + Bf_{k-1} + C\delta_k$.

We write inequality (3.17) in terms of linear operator $\mathcal{M} := (\epsilon(d)A + B)$ as

$$f_k \leq \mathcal{M}f_{k-1} + C\delta_k.$$

Using the Lemma 3.3 as before, we get to

$$f_k \leq \mathcal{M}^k f_0 + \sum_{i=0}^{k-1} \mathcal{M}^{k-i} C\delta_i. \quad (3.22)$$

We already know from equation (3.20) that $\|\mathcal{M}^k f_0\|_\infty \leq C\|f_0\|_\infty e^{k(V-1)}$, so that we can take norm infinity in equation (3.22) and then write it as

$$\|f_k\|_\infty \leq Ce^{k(V-1)}\|f_0\|_\infty + C^2 \sum_{i=0}^{k-1} e^{(k-i)(V-1)}\|\delta_i\|_\infty. \quad (3.23)$$

Then, the condition to obtain convergence to 0 of f_k as $k \rightarrow \infty$ is given by two different requirements. First, as before, condition (3.21) should be satisfied. Secondly, $\|\delta_k\|_\infty$ has to converge to 0 as $k \rightarrow \infty$, as proven in Theorem 2.9. \square

Remark 3.6. Convergence to the equilibrium was also proven using the entropy method in [29, Theorem 5.3] in weakly connected networks. In particular, the required smallness of the connectivity parameter was $8b^2e^{\lambda d} \leq \epsilon/N_\infty$, for ϵ a small constant, depending on N_∞ and constants of Sobolev injection of $H^1(I)$ in $L^\infty(I)$ (I is a small neighbourhood of V_R). Our bound is $b^4 < \lambda/\hat{C}$. With this strategy we obtain the convergence for any large d if the smallness of b is satisfied. This could also be compared to a similar result in [43, Theorem 4.1].

4 Numerical results: Global perspective on the long-time behaviour of the delayed NNLIF model

In this section we illustrate numerically the relationship between the discrete pseudo equilibrium model (2.2) and the highly delayed NNLIF model (1.2). We give numerical evidence that the long-time behaviours of the two models are closely related. In particular, in the long run, we can predict the behaviour of the nonlinear system by knowing the behaviour of the discrete system, which was studied in Section 2.

The numerical approximation of equation (1.2) has been carried out by means of a fifth order finite difference flux-splitting WENO scheme [46] for the advection term, a standard second order finite differences for the diffusion term, and an explicit third order TVD Runge-Kutta method for the time evolution. This scheme has been used previously to simulate NNLIF models [28] and a detailed explanation of the scheme can be found in [2]. Other numerical schemes, such as those based on a Scharfetter-Gummel reformulation, have also been used to carry out numerical simulations of this model [30, 32].

Our discretisation is composed of a mesh in voltage with $v_i = v_{min} + i\Delta v$, $i = 0, 1, 2, \dots, n_v$ with a suitable minimum value v_{min} , which ensures the mass is approximately 0 to the left of v_{min} ; and a threshold value V_F as the maximum mesh value v_{n_v} . The mesh in time is given by $t_j = j\Delta t$, $j = 0, 1, 2, \dots, n_t$ where the value of Δt is chosen so that it complies with the CFL condition imposed for a correct approximation of the drift and diffusion terms

$$\Delta t < \min \left(\frac{a(\Delta v)^2}{2}, \frac{C_{CFL}\Delta v}{\max |bN(t-d) - v|} \right).$$

The reset value V_R is one of the nodes of the mesh in voltage, and the delta function in the right term of (1.2) is approximated by a very sharp Maxwellian centered in V_R , of the form:

$$m(x) = \frac{1}{\sqrt{2\pi}\sigma} e^{-\frac{(x-V_R)^2}{2\sigma^2}}, \quad (4.1)$$

with $\sigma = 10^{-6}$, which is normalized by integrating it in our mesh and setting the integral to 1. The boundary conditions are imposed at every time step by setting $p(v_0) = 0$ and $p(v_{n_v}) = 0$. Furthermore, we ensure that the values of the probability distribution near v_0 are numerically 0, so that there are no issues arising from forcing the boundary condition with the size of the mesh.

The initial conditions we have considered for these simulations are approximations of:

- The pseudo-equilibria profiles (see (2.2))

$$p(v) = \bar{N} e^{-\frac{(v,bN)^2}{2}} \int_{\max(v,V_R)}^{V_F} e^{\frac{(w-bN)^2}{2}} dw, \quad (4.2)$$

fulfilling the condition $\int_{-\infty}^{V_F} p(v) dv = 1$, with the particular cases

$$p^-(v) = N^- e^{-\frac{(v-bN^+)^2}{2}} \int_{\max(v,V_R)}^{V_F} e^{\frac{(w-bN^+)^2}{2}} dw, \quad N^- = \frac{1}{I(N^+)} \quad (4.3)$$

and

$$p^+(v) = N^+ e^{-\frac{(v-bN^-)^2}{2}} \int_{\max(v, V_R)}^{V_F} e^{-\frac{(w-bN^-)^2}{2}} dw, \quad N^+ = \frac{1}{I(N^-)}, \quad (4.4)$$

the 2-cycle of pseudo-equilibria sequence, given by the 2-cycle $\{N^-, N^+\}$ of the firing rate sequence.

- Double Maxwellians:

$$\frac{1}{\sqrt{8\pi\sigma}} \left(e^{-\frac{(v-\mu)^2}{2\sigma^2}} + e^{-\frac{(v+\mu+2)^2}{2\sigma^2}} \right) \quad \mu \in \mathbb{R}, \sigma > 0. \quad (4.5)$$

Three system parameters are fixed: $a = 1$, $V_R = 1$ and $V_F = 2$. The connectivity parameter b and the delay d will change depending on the simulation, displaying different phenomena for this model.

We analyse in detail three different aspects: bi-stability between the lower equilibrium and the plateau distribution for excitatory networks with two equilibria; the emergence of periodic solutions for highly inhibitory systems; and the influence of the delay value on the evolution in time of the nonlinear system, in relation with the behaviour of the pseudo-equilibria sequence. The rest of the system behaviour is well represented by the above study, as we shall explain below.

The case with two equilibria: Bi-stability between the lower equilibrium and the plateau distribution

We consider in this case the regime in which the implicit equation $NI(N) = 1$ has two solutions ($N_1^* < N_2^*$), which determine the stationary firing rates of the nonlinear system (1.2). This regime corresponds to values of the connectivity parameter b between $V_F - V_R = 1$ and approximately 2.3. Specifically, we take $b = 1.5$ for which $N_1^* \approx 0.194$ and $N_2^* \approx 2.294$, but we emphasise that other values of b in that range appear to show an equivalent behaviour. For this connectivity value, Figure 5 shows the firing rate sequence $N_{k,\infty}$ (see (2.1)) for different initial conditions $N_{0,\infty}$. The behaviour of the sequence was analysed in Theorem 2.3. Thus, we know that in that case (with two equilibria) the firing rate sequence tends to N_1^* or diverges, as we can see in Figure 5.

In Figure 6 we show that the behaviour of the discrete system is reproduced for the nonlinear system. It is determined by the value of the initial firing rate

$$N_0 := -\partial_v p_0(V_F),$$

depending on the position with respect to N_1^* and N_2^* . The threshold value between both regimes is $N_2^* \approx 2.294$: for a lower value of N_0 the nonlinear system is seen to

converge to N_1^* , while for $N_0 > N_2^*$, the firing rate seems to diverge.

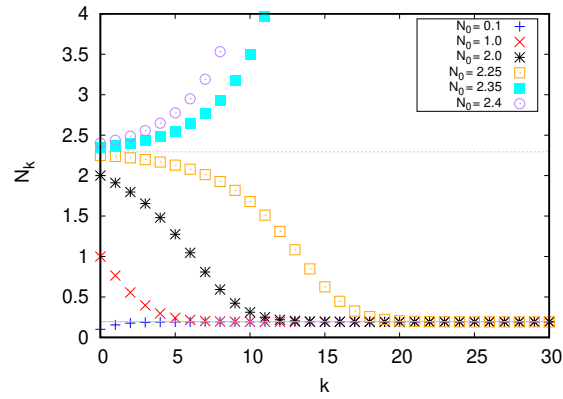


Figure 5: Firing rate sequence $N_{k,\infty}$ (2.1) with $b = 1.5$ and different values of initial condition $N_{0,\infty}$. Solid and dashed straight horizontal lines represent equilibria N_1^* and N_2^* respectively.

In Figure 6 we consider two different initial conditions of the type (4.2), with the respective values of $N_0 = 2.233348$ and $N_0 = 2.365824$, which serve as representatives of two different regimes for the delayed nonlinear system: convergence to the low steady state or formation of the plateau distribution, when considering transmission delay $d = 10$. This illustrates bi-stability between the low steady state and the plateau distribution, depending only on the initial condition (see [37] for a better understanding of the plateau distribution). As we also mention in [37], no matter what the size of the delay is, we shall find that the nonlinear system seems to behave according to the pseudo-equilibria sequence. This appears to indicate that the long-term behavior of the system can be decided only on the basis of the value of N_0 . In the upper graphs, we see the time evolution of the firing rates and on the bottom, we see the shape of the voltage distributions at the end of the two simulations ($t = 220$). When the system starts with an initial condition whose N_0 is less than N_2^* , the firing rate converges to N_1^* (left plot). However, if the system starts with $N_2^* < N_0$, then $N(t)$ increases in time (right plot). This behaviour is consistent with that of the firing rate and pseudo-equilibria sequences described in Theorem 2.3; if $N_{0,\infty} = N_0$ is below the high stationary firing rate N_2^* then $\{N_{k,\infty}\}_{k \geq 0}$ converges to the lower one N_1^* , and, if $N_{0,\infty} = N_0$ is higher than N_2^* then $\{N_{k,\infty}\}_{k \geq 0}$ diverges.

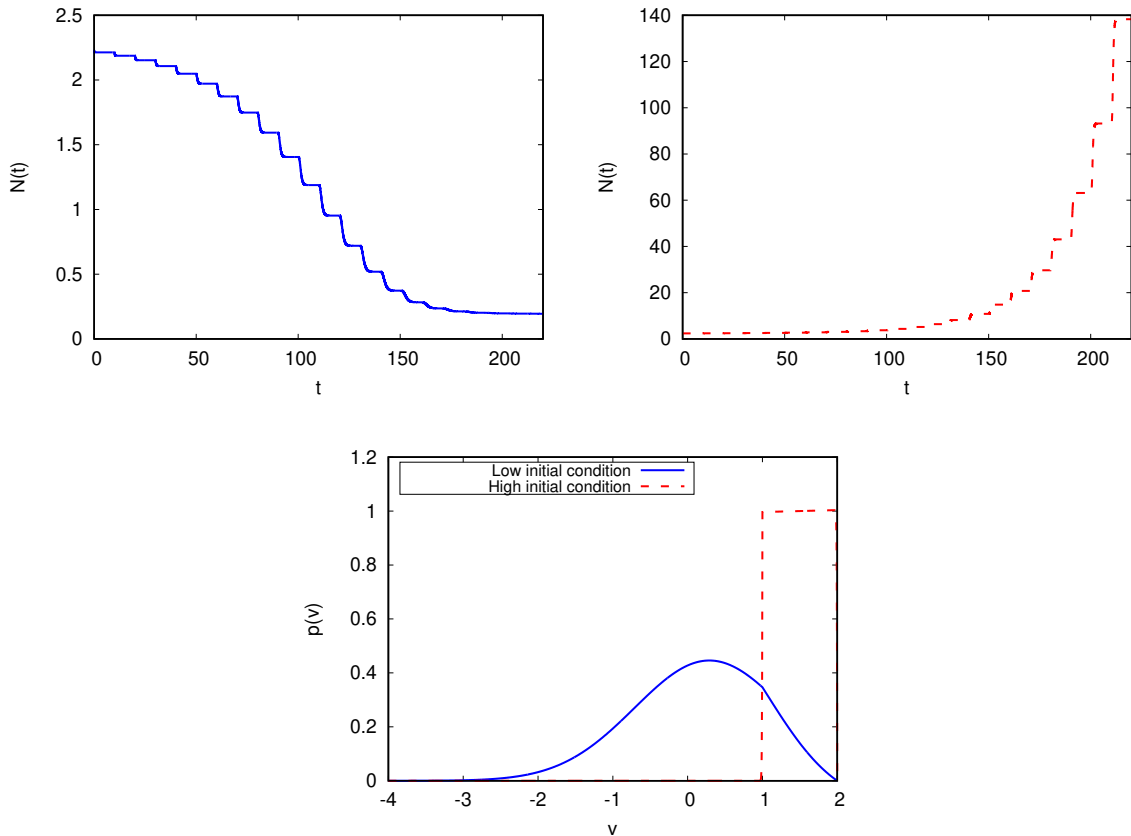


Figure 6: **Nonlinear system (1.2) with $b = 1.5$ and $d = 10$.**

Top: Evolution on time of the firing rate, $N(t)$, with initial conditions given by equation (4.2) with $N = 2.25$, $\bar{N} = 2.233348$, chosen to be smaller than N_2^* (left) and $N = 2.35$, $\bar{N} = 2.365824$, greater than N_2^* (right).

Bottom: Comparison of distributions $p(v, t)$ at the end of the simulations ($t = 220$).

We have compared the discrete and the nonlinear systems in Figure 7. Here we have used the same simulations shown in Figure 6 for the nonlinear system, and we have calculated the sequences $\{N_{k,\infty}\}_k$ and $\{p_{k,\infty}\}_k$ by starting with the same initial condition as for the simulations, $N_{0,\infty} = N_0 = 2.233348$ in the left plots and $N_{0,\infty} = N_0 = 2.365824$ in the right ones. In the top plots we observe the comparison between $N(t)$ and $\{N_{k,\infty}\}_k$ until $t = 200$, while in the bottom plots we show the comparison between $p(v, t = 20)$, $p(v, t = 120)$ and the pseudo-equilibria $p(v, t = 200)$ with $p_{2,\infty}(v)$, $p_{12,\infty}(v)$ and $p_{20,\infty}(v)$ respectively. We can observe that the delay $d = 10$ is large enough so that the simulation results, both $p(v, t)$ and $N(t)$, almost completely coincide with the elements of the pseudo equilibrium and firing rate sequences starting from the same initial condition.

In [29] a global existence theory was developed for the nonlinear system (1.2) with a transmission delay $d > 0$, by extending the results of [25]. So the sequence of pseudo-equilibria suggests that the firing rate of the nonlinear system should diverge and the theory tells us that this cannot happen in finite time. The only possibility is then that $N(t)$ diverges in infinite time, giving rise to the plateau distribution as $N(t)$ grows. This is precisely the behaviour seen in our simulations.

So that in cases where the firing rate sequence diverges, we expect the following to be true: *Let us consider $0 < b$, an initial condition $p_0 \in X$ (and $N(t) = -\partial_v p_0(V_F)$ for $t \in [-d, 0]$) and p its related solution to the nonlinear system (1.2). Assuming that the firing rate sequence $\{N_{k,\infty}\}_{k \geq 0}$, with initial value $N_{0,\infty} := -\partial_v p_0(V_F)$ (see (2.1)) diverges, then the solution, p , to the nonlinear system (1.2) with transmission delay $d > 0$ and initial condition p_0 evolves to a plateau distribution, i.e, the membrane potential of the system tends to be uniformly distributed between V_R and V_F .*

The numerical results in Figures 5 and 6 and numerical experiments in the literature also illustrate the behaviour of the nonlinear system when the firing rate sequence converges. Theorems 2.3 and 2.5 give conditions on the initial value of the firing rate sequence to converge to an equilibrium of the system (in both cases, excitatory and inhibitory). In Figures 6 and 7 we see that the nonlinear system tends to an equilibrium when the discrete system also tends to equilibrium. In the following experiments below we shall see it for the inhibitory case and in [24, 28, 30, 37] it can also be seen for the excitatory case with only one equilibrium.

So that in case where firing rate sequence converges, we expect the following to be true: *Let us consider $b \in \mathbb{R}$, an initial condition $p_0 \in X$ (and $N(t) = -\partial_v p_0(V_F)$ for $t \in [-d, 0]$) and p its related solution to the nonlinear system (1.2). Assuming that the firing rate sequence $\{N_{k,\infty}\}_{k \geq 0}$, with initial value $N_{0,\infty} := -\partial_v p_0(V_F)$ (see (2.1)) converges to $N_\infty > 0$, then there exists $d_0 > 0$ large enough and $Q, \mu > 0$, such that the solution, p , to the nonlinear system (1.2) with transmission delay $d > d_0$ and initial condition p_0 fulfills*

$$\|p(\cdot, t) - p_\infty(\cdot)\|_X \leq Qe^{-\mu t} \|p_0 - p_\infty\|_X \quad \forall t \geq 0, \quad (4.6)$$

where p_∞ is the stationary solution to the nonlinear system (1.2) with firing rate N_∞ .

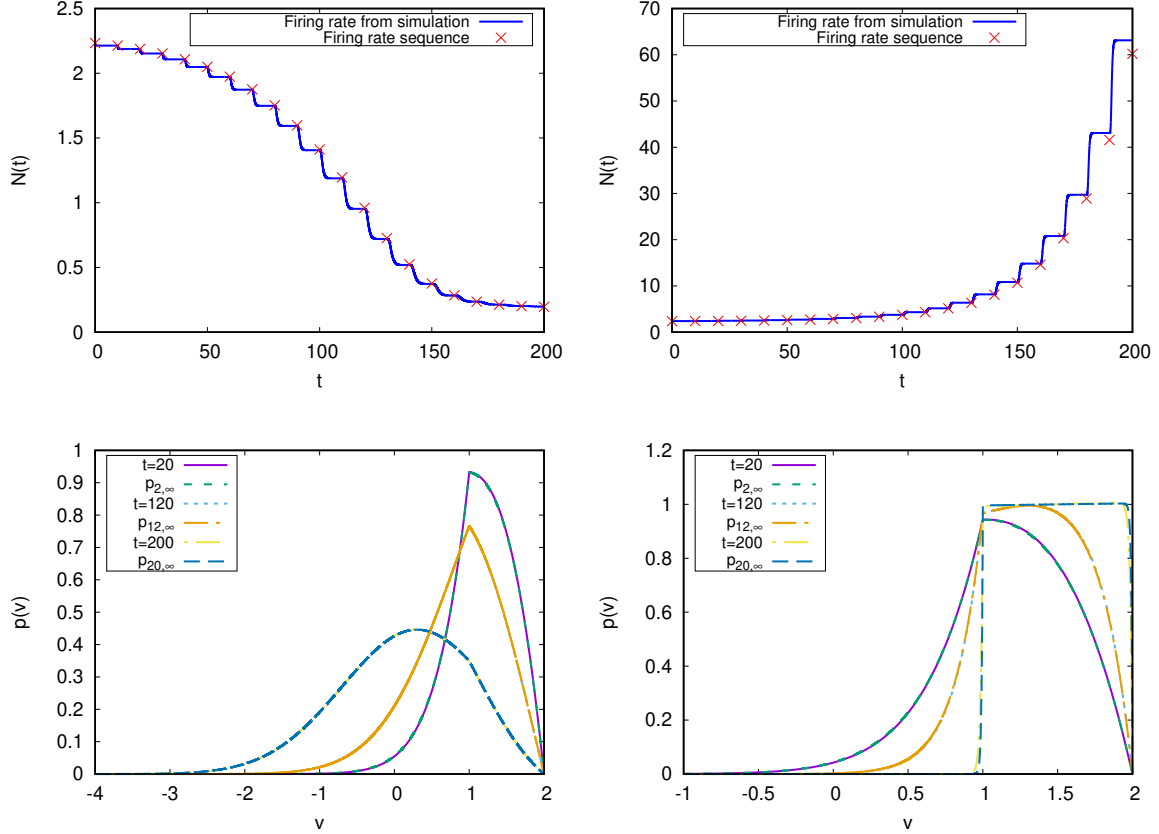


Figure 7: **Comparison between the nonlinear system (1.2) and the discrete system with $b = 1.5$ and $d = 10$.** *Top:* Comparison between the firing rate of the approximated solution to the nonlinear equation, $N(t)$ and the sequence of firing rates $N_{k,\infty}$. *Bottom:* Solutions of the nonlinear problem, $p(v, t)$ at different times, compared with the pseudo-equilibria $p_{k,\infty}(v)$ which correspond to those times. *Left:* initial condition given by equation (4.2) with $N = 2.25$, $\bar{N} = 2.233348$, chosen to be smaller than N_2^* . *Right:* initial condition given by equation (4.2) with $N = 2.35$, $\bar{N} = 2.365824$, greater than N_2^* .

Influence of the delay value on the excitatory nonlinear system behavior: cases with one equilibrium and without equilibria

In this subsection we show results concerning the influence of the delay value on the behavior of the nonlinear system. As we said before, the nonlinear system must follow the behavior of the pseudo-equilibrium sequence when the delay is sufficiently large. Although deciding when the delay is large enough depends on the parameters of each simulation (especially depends on b and the initial condition of the firing rate N_0). To evaluate the influence of the delay on the nonlinear system we will use two situations where at least numerically the behavior of the nonlinear system is well known. The first is the case with $b = 0.5$ and therefore a single equilibrium, where we know that, if we consider any delay $d > 0$ the system converges to its unique equilibrium. The second is the case $b = 2.2$, where there are no equilibria and we know that any system with delay tends to a plateau distribution, i.e., its firing rate grows in time but does not diverge in finite time.

Therefore we will see how the use of different values for the delay d does not change the fundamental long-term behavior of the system, but makes the system in each delay interval converges to the corresponding pseudo-equilibrium or not. Considering that there is only one possible long-term behavior for each case, we will consider a single initial condition in each case and different values for the delay.

First, in Figure 8 we observe the sequence of firing rates for both values of b , which behave as mentioned before for the nonlinear system with delay: for $b = 0.5$, it converges to the unique equilibrium regardless of the initial condition; for $b = 2.2$, it increases in time. In Figure 9 we show the evolution on time of the firing rate of the nonlinear system, $N(t)$, with three different values of the delay. In the left plot, considering $b = 0.5$, we note the need for a large delay (at least greater than 2) for the nonlinear system to pass one by one through the pseudo-equilibria and even remain close to them for some time. However we note from the right plot of Figure 9 the lower requirement of high delay values to observe the nonlinear system stabilizing for a certain time in the pseudo-equilibria, the necessary value being somewhere between 0.1 and 1.

If we consider these results together with those shown in the previous subsection for $b = 1.5$, we notice an influence of the value of b on the value of d necessary for the system to pass through its associated pseudo-equilibria. So that the smaller the value of b is, the greater the value of d should be. This consideration is in accordance with the stated in the proof of Theorem 3.1 (see (3.21)).

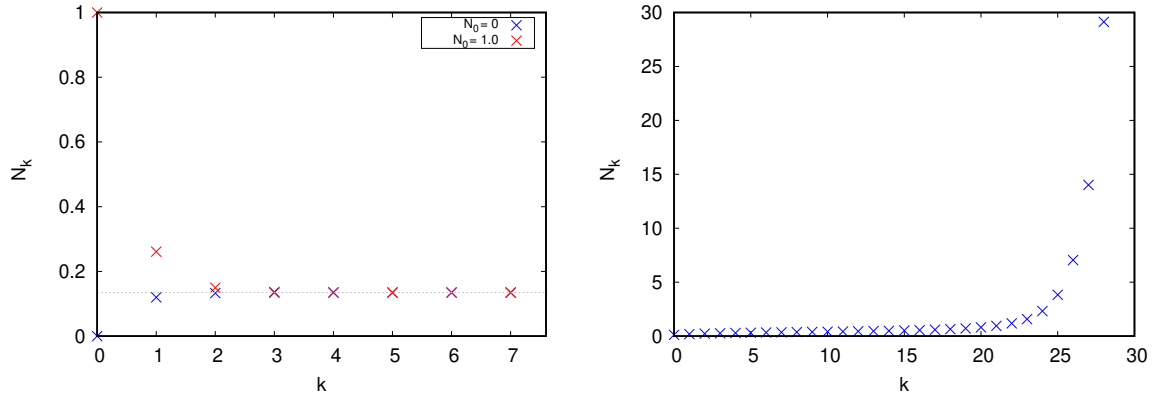


Figure 8: **Firing rate sequence $N_{k,\infty}$ (2.1) with $b = 0.5$ and $b = 2.2$.**

Left: $b = 0.5$ and different values of initial condition $N_{0,\infty}$ below and above the unique equilibrium (gray dashed line). *Right:* $b = 2.2$. This is a case without equilibria.

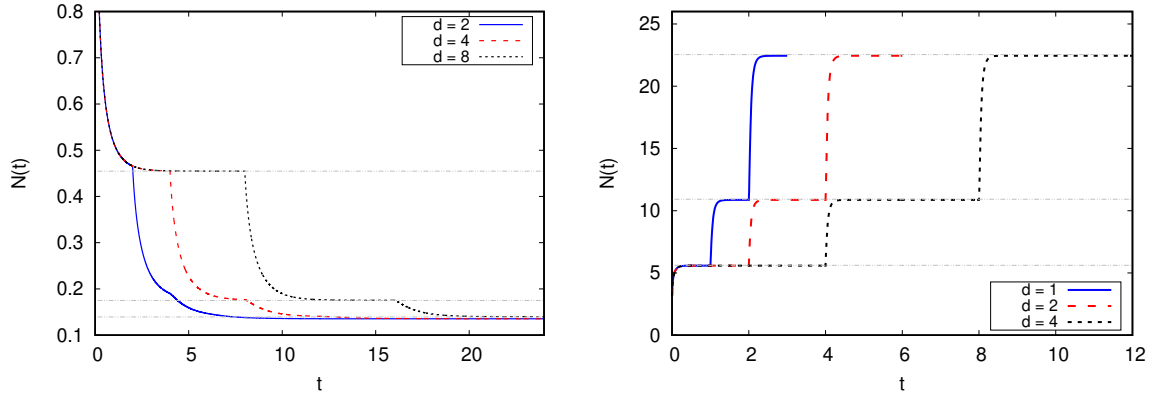


Figure 9: **Time evolution of the firing rate, $N(t)$, for the nonlinear system (1.2) with different values of the delay and the connectivity parameter.**

Left: $b = 0.5$ and different values of delay. Initial conditions are given by equation (4.2) with $N = 6$. In this case there is unique equilibrium. *Right:* $b = 2.2$ and different value of the delay. Initial conditions are given by equation (4.2) with $N = 2$. For each delay value d , the plot shows the firing rate in a time range $[0, 3d]$. This is a case without equilibria. In both plots dashed lines correspond with values of the firing rate sequence (2.1) with b and $N_{0,\infty}$ (initial condition) given by the parameters of the nonlinear system.

Periodic states in the highly inhibitory case with large delay

In this second experiment we discover conditions under which periodic solutions appear in an inhibitory system. This phenomenon was observed numerically in [32]. We have determined the value of parameter b for which the periodic states appear for large delay, in the light of the behaviour of the sequence of pseudo-equilibria. Here we find an important difference with the excitatory case, where the size of the delay is not essential to determine whether the long-term behavior of the system conforms to that described by the pseudo equilibrium sequence. For highly inhibitory systems the size of the transmission delay is key. We recall that for the inhibitory case the nonlinear system has only one steady state p_∞ , with its associated stationary firing rate N_∞ , and the behaviour of the firing rate sequence $N_{k,\infty}$ (the discrete system) is given by Theorem 2.5: $N_{k,\infty}$ tends to the equilibrium or to 2-cycle.

Our first aim is to find appropriate values of the parameters for which periodic states emerge. Then we shall focus on the study of periodic solutions. Figure 10 suggests which values we should choose for b in order to find periodic states. We see that the bifurcation value b^* is around the value $b^* \approx -9.4$ (in the sense of Theorem 2.5). Thus, the firing rate sequence $N_{k,\infty}$ converges to N_∞ if $b^* < b$ and tends towards a 2-cycle $\{N^-, N^+\}$, if $b < b^*$. This tells us that a sufficiently large delay will allow us to observe the same behavior when simulating the nonlinear system. We must emphasize that for all cases with $b \leq 0$, the choice of initial condition $N_{0,\infty}$ does not appear to change the long-term values of the firing rate sequence $N_{k,\infty}$.

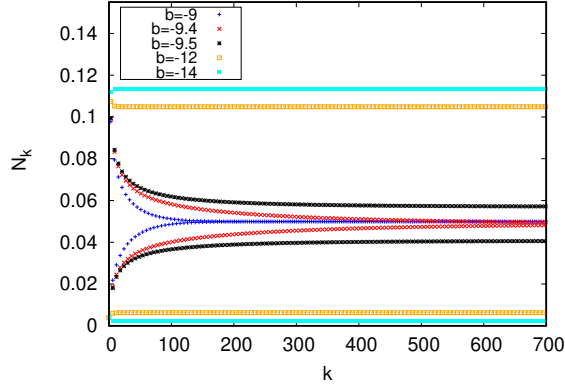


Figure 10: **Firing rate sequence $N_{k,\infty}$ (2.1) for different values of $b < 0$ with $N_{0,\infty} = 0.004$. For $b < -9,4$ the sequence tends towards a 2-cycle.**

Due to the numerical study of the firing rate sequence, we have a good guess for the values of b needed to find periodic states. Let us test different values of b and d and observe the behavior of the nonlinear system. The following simulations have been performed using as initial condition the profile given by Equation (4.2), with $N = 0$, letting the system evolve up to $t = 300$. In the left plot of Figure 11 we show the firing rate $N(t)$ of the nonlinear system, with delay $d = 10$, testing three different values of b to find stable oscillations. For b not sufficiently negative, the amplitude of the oscillations is observed to be damped in time, suggesting a tendency towards the single steady state of the system, as we showed earlier in the study of the sequence of pseudo-equilibria (see Theorem 2.5). For a sufficiently negative value of b , as shown for $b = -12$, we observe fairly stable oscillations in time. Thus, to be sure of the stability of the solutions without the need for an excessively large delay, we will choose $b = -14$ for the following experiments. In the right plot of Figure 11 we can see, for $b = -14$, how the choice of a large enough delay permits the system to evolve towards a periodic state. This picture shows the evolution in time of the firing rate $N(t)$ with different delay values d . If d is small ($d = 2$) the firing rates tends to a stationary value, while if d is large ($d = 10, d = 25$), its behaviour tends to be periodic. We must emphasize that, when we do not set a sufficiently high delay, even if the value of b is very negative and therefore the pseudo-equilibria sequence in Theorem 2.5 points to periodic behavior, we shall observe convergence to the steady state, as it is shown with solid line in the right graph, for $d = 2$. This is a strong difference between the inhibitory case with periodic state and the excitatory case with plateau state, where the size of the delay was irrelevant.

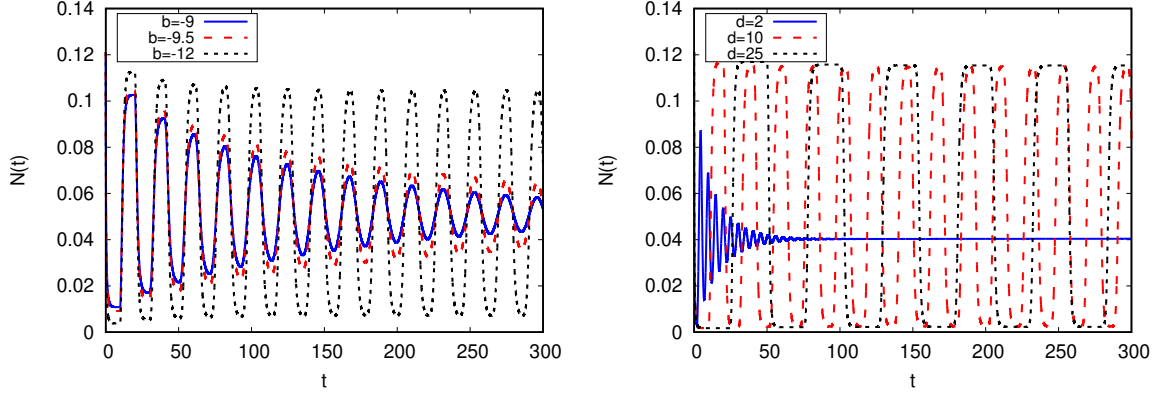


Figure 11: **Nonlinear system** (1.2) Time evolution of the firing rate, $N(t)$. The initial condition is given by equation (4.2) with $N = 0$.

Left: Different values of the connectivity parameter b with delay $d = 10$. *Right:* Connectivity parameter $b = -14$ with different values of the delay.

To study the periodic solutions of the highly inhibitory nonlinear system, we shall set $b = -14$ and $d = 25$ for the rest of the simulations.

For these parameters, the steady state of the nonlinear system $p_\infty(v)$ has firing rate $N_\infty = 0.0396$. When we study numerically the firing rate sequence $N_{k,\infty}$ we find a tendency towards the values $N^- = 0.0022$ and $N^+ = 0.1136$ in the sense of Theorem 2.5, as shown above in Figure 10 for $b = -14$.

In Figure 12 we compare the solution to the nonlinear system (1.2) with the 2-cycle, $\{p^-(v), p^+(v)\}$, found in Theorems 2.5 and 2.11 for the succession of pseudo-equilibria $\{p_{k,\infty}\}_{k \geq 0}$. In the left graph we observe the comparison between the lower state $p^-(v)$ and the approximated solution to the Fokker-Planck equation, starting with an initial condition given by an approximation of $p^-(v)$. The times shown in the graphs have been selected so that the distribution should coincide with $p^-(v)$, since they are even multiples of the delay. In the graph on the right we see a similar comparison between $p^+(v)$ and the approximated $p(v)$, starting now with an approximation of $p^+(v)$, also in the times they should overlap. We can see that in the left graph there is a small difference between the values of $p(v, t)$ for the different times represented with respect to $p^-(v)$, but in the right graph the difference is practically negligible. This may be due to the fact that the observed period for the periodic state is not exactly $2d$, as can be seen in the bottom plot, where we show the firing rate of the system, computed for a simulation with initial condition given by Equation (4.2) with $N = 0$.

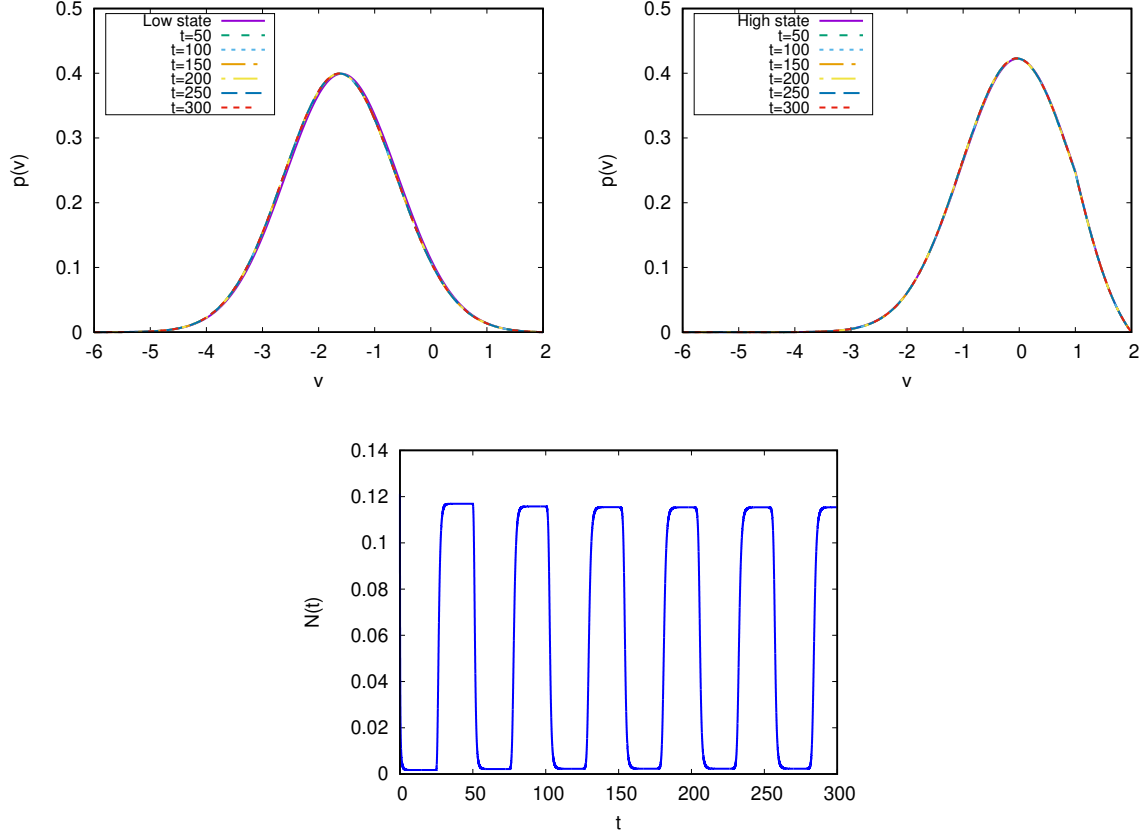


Figure 12: **Nonlinear system (1.2) with $b = -14$ and delay value $d = 25$.**

Top left: Initial condition given by the pseudo equilibrium $p^-(v)$, from equation (4.3). Approximated solution to the nonlinear system, $p(v, t)$, at different times, compared with $p^-(v)$. *Top right:* Initial condition given by the pseudo equilibrium $p^+(v)$, from equation (4.4). Approximated $p(v, t)$ at different times, compared with $p^+(v)$. *Bottom:* Initial condition given by (4.2) with $N = 0$. Time evolution of the firing rate $N(t)$.

Finally, in Figure 13, we analyse how the initial condition influences the evolution of the nonlinear system. We consider four different initial conditions shown in the top left graph: $p^-(v)$, $p^+(v)$ and two double Maxwellians distributions, as (4.5), with $\mu_{\text{low}} = -1$, $\mu_{\text{high}} = 0.4$ and $\sigma = 0.5$ in both cases. Our purpose is to provide evidence that regardless of the initial condition, with these values of b and d , the system will end up in a periodic state between the pseudo-equilibria $p^-(v)$ and $p^+(v)$, with pseudo-stationary firing rates N^- and N^+ . Nevertheless, it is worth noting how the initial condition determines which pseudo equilibrium is going to be reached first, determining the times at which the distribution $p(v, t)$ will be close to $p^-(v)$ and $p^+(v)$.

In top right plot of Figure 13, we can see the evolution on time of the four firing rates of the different simulations. We note that for $t > 150$ the firing rates of the simulations starting with the low state and the double Maxwellians low ($\mu_{\text{low}} = -1$) are synchronised, and the same is true for the firing rates of the simulations starting with the high state and the double Maxwellians high ($\mu_{\text{high}} = 0.4$). We also see, in the bottom graphs, these synchronies of the corresponding distributions $p(v, t)$, “passing” through $p^-(v)$ and $p^+(v)$ at the same times ($t = 250$ left and $t = 264$ right), and describing, in this way, a periodic behaviour.

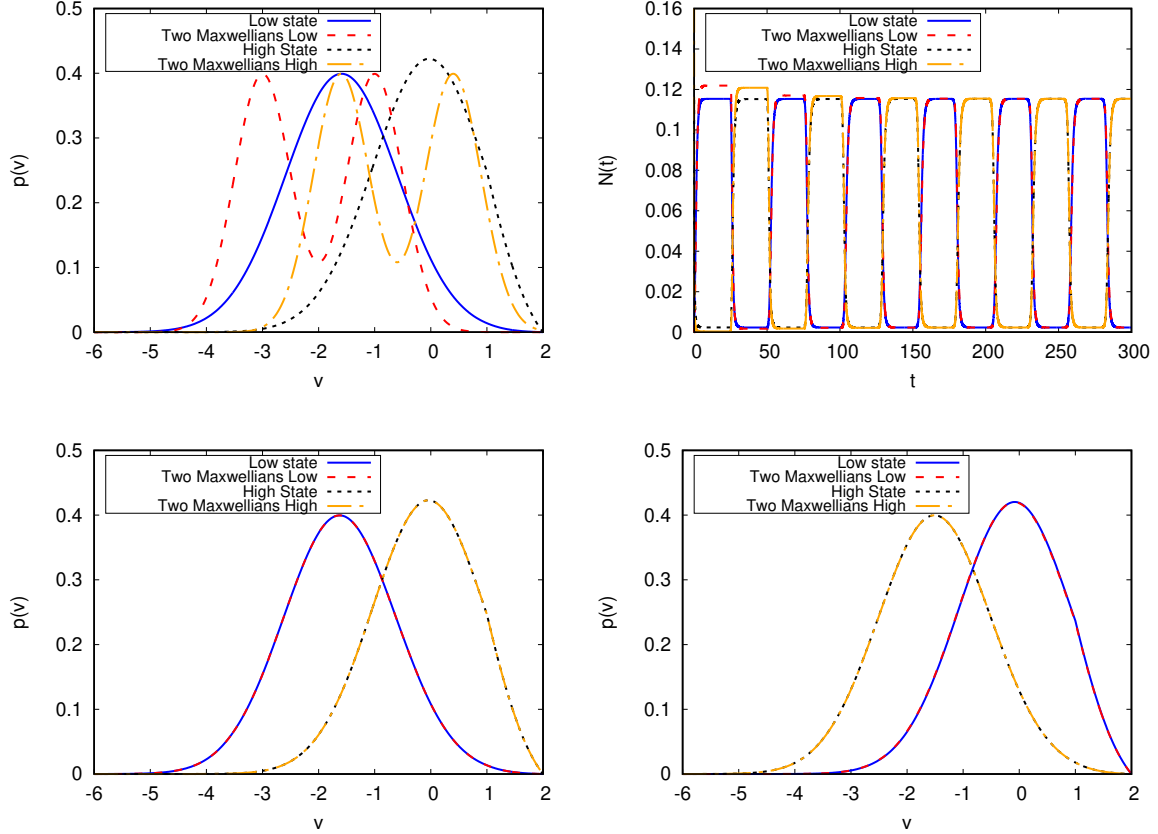


Figure 13: **Nonlinear system (1.2) with $b = -14$ and $d = 25$** using four different initial conditions. *Top left:* Initial conditions: we consider the low pseudo equilibrium given by equation (4.3), the high pseudo equilibrium given by equation (4.4) and two configurations of double Maxwellians given by equation (4.5), with $\mu_{\text{low}} = -1$, $\mu_{\text{high}} = 0.4$ and $\sigma = 0.5$ in both cases. *Top right:* Comparison between the time evolution of the firing rate $N(t)$ depending on the initial condition. *Bottom left and right:* Distribution $p(v)$ at times $t = 250$ and $t = 264$ respectively, for both initial conditions.

The behaviours shown in Figures 11 and 12 agree with that of the firing rate and pseudo-equilibria sequences described in Theorems 2.5 and 2.11; if $b^* \approx 9.5 < b < 0$ we find convergence to the steady state, no matter what the initial condition is. If $b < b^*$ then d should be sufficiently large to find a periodic state. Otherwise, there will be convergence to equilibrium. Finally, Figure 13 helps us to understand which are the different options for the possible periodic states to which the nonlinear system tends, as well as their dependence on the initial condition.

The periodic states seem to be determined by the solutions starting from one of the two pseudo-equilibria. These solutions, when the delay is large, approach the other pseudo equilibrium at the end of each delay period. In the next delay period they return to the initial pseudo equilibrium, and so continue in the following periods of length d . And they tend to a periodic state, which we can call $p_{\infty}^{-}(v, t)$ and $p_{\infty}^{+}(v, t)$, depending if the initial condition is $p^{-}(v)$ or $p^{+}(v)$, respectively. Simulations lead us to suspect that the period is $2d + \epsilon$, because of the time it takes to move from one pseudo equilibrium to another, and $p_{\infty}^{-}(v, t) = p_{\infty}^{+}(v, t + d + \epsilon/2)$.

To be more precise what we would expect to be demonstrated in the nonlinear

system, in cases where the firing rate sequence tends to 2-cycle, i.e $b < b^*$, can be stated as follows: *Let us consider $b < 0$, an initial condition $p_0 \in X$ (and $N(t) = -\partial_v p(V_F)$ for $t \in [-d, 0]$) and p its related solution to the nonlinear system (1.2). Assuming that the firing rate sequence $\{N_{k,\infty}\}_{k \geq 0}$, with initial value $N_{0,\infty} := -\partial_v p_0(V_F)$ (see (2.1)) tends to a 2-cycle, $\{N^-, N^+\}$, then there exist $d_0 > 0$ large enough, such that the solution, p , to the nonlinear system (1.2) with transmission delay $d > d_0$ and initial condition p_0 has the following behaviour:*

1. *If the initial datum, p_0 , is p^- , the pseudo-equilibrium of the nonlinear system (1.2) associated to N^+ (see (4.3)), thus, the solution tends to a periodic function, $p_\infty^-(v, t)$.*
2. *If the initial datum, p_0 , is p^+ , the pseudo-equilibrium of the nonlinear system (1.2) associated to N^- (see (4.4)), thus, the solution tends to a periodic function, $p_\infty^+(v, t)$.*
3. *For a general initial condition $N_0 := -\partial_v p_0(V_F)$:*
 - (a) *If $N_0 < N_\infty$, thus, the system tends to $p_\infty^-(v, t + \delta_{N_0})$.*
 - (b) *If $N_\infty < N_0$, thus, the system tends to $p_\infty^+(v, t + \delta_{N_0})$,**with fixed $\delta_{N_0} \in \mathbb{R}$ for each initial condition N_0 .*

5 Conclusions

In this article we have introduced a discrete system which helps to better understand the nonlinear leaky integrate and fire (NNLIF) model when large transmission delay is considered. This discrete system is defined only in terms of the system parameters. It allows us to build a firing rate and pseudo-equilibria sequences, that determine the long-time behaviour of the nonlinear system (1.2). The advantage of the discrete model lies in its simplicity. It allows for quick simulations that provide accurate information about the NNLIF system, such as the estimated time to approach equilibrium, whether the system tends toward a steady state, the possible appearance of periodic solutions or plateau states, etc.

We have analytically studied the related discrete system. Our results give a global view of the asymptotic behaviour of the discrete system for all possible values of the connectivity parameter b . Analytically, the link with the nonlinear system (1.2) has been proved in Theorem 3.1, but it only works if b is small enough, in which case the system converges to its unique equilibrium. The long-term behaviour for weakly connected networks was already known using the entropy dissipation method [27,29,40]. However, our strategy is different and new, as it describes the behaviour in relation to the pseudo-equilibria sequence (2.2).

In addition to our analytical results we show a numerical study, that leads us to think that the nonlinear system should behave as shown by the sequence of pseudo-equilibria in all cases with high delay. The motivation for that conjecture is clear: large delay means that the nonlinear system is piecewise linear and with enough time to reach linear equilibria. The numerical results of this work describe the existence of periodic states for the nonlinear system, in the case of large delay and very negative

connectivity parameter, as has been observed previously by other authors [32]. We offer range of values for the parameters b and d from which this phenomenon should occur. Moreover, we can link the numerical part with our study of the sequence of pseudo-stationary states, giving a plausible theoretical explanation for the existence of these oscillations, and shedding some light on the subsequent analytical test of them, which will be carried out in future work. We can also relate the study of the sequence of pseudo-equilibria to the behaviour of the system for b positive. Finding here a possible explanation for the emergence of the plateau state, observed in the previous work [37].

To conclude, we summarise the observed global behaviour of systems with large delay in terms of its initial firing rate, $N_0 = -\partial_v p_0(V_F)$:

1. Excitatory networks ($0 < b$) show two possibilities: they can evolve to:
 - (a) a stationary distribution, the single steady state or the steady profile with lower firing rate, in case of two equilibria.
 - (b) the uniform distribution between V_R and V_F (plateau state). This case could occur even with small transmission delay value, d , if there is no steady state (b large), and in cases with two equilibria.
2. Inhibitory networks ($b < 0$) also show two possibilities: they can evolve towards:
 - (a) the stationary distribution, if $b^* < b$.
 - (b) a periodic solution between the 2-cycle $\{p^-, p^+\}$, if $b < b^*$.

A Appendix: Auxiliary calculations

We study the monotonicity of the function $g(b) = \frac{-\partial_N I(b, N_b^*)}{I(b, N_b^*)^2}$, used in the proof of Theorem 2.5.

Lemma A.1. *Let us consider $b \in (-\infty, 0]$ and $N(b)$ the solution to the equation $NI(b, N) = 1$, then, $g(b) := \frac{-\partial_N I(b, N(b))}{I(b, N(b))^2}$ is an increasing function, defined in $(-\infty, 0]$.*

Proof. We consider $v(s) := s^{-1} e^{-s^2/2} e^{-sbN(b)} (e^{sV_F} - e^{sV_R})$, $w(s) := e^{-s^2/2} e^{-sbN(b)} (e^{sV_F} - e^{sV_R})$ and $u(s) := s e^{-s^2/2} e^{-sbN(b)} (e^{sV_F} - e^{sV_R})$, and rewrite the function $I(b, N(b))$ and some of its useful derivatives as follows:

$$I(b, N(b)) = \int_0^\infty v(s) ds > 0,$$

$$\partial_N I(b, N(b)) = -b \int_0^\infty w(s) ds > 0, \quad \partial_b I(b, N(b)) = -N(b) \int_0^\infty w(s) ds < 0,$$

$$\partial_N^2 I(b, N(b)) = b^2 \int_0^\infty u(s) ds > 0, \quad \text{and } \partial_b \partial_N I(b, N(b)) = bN(b) \int_0^\infty u(s) ds - \int_0^\infty w(s) ds < 0,$$

In the following, to shorten the notation we write I instead of $I(b, N(b))$, N instead of $N(b)$ and N' instead of $\frac{dN}{db}(b)$. Thus

$$g'(b) = \frac{-I \partial_b \partial_N I - N' I \partial_N^2 I + 2 \partial_N I \partial_b I + 2N' (\partial_N I)^2}{I^3}. \quad (\text{A.1})$$

We derive implicitly in $I(b, N(b))N(b) = 1$, and obtain $N' = \frac{-\partial_b I}{I^2 + \partial_N I}$. Using it in (A.1)

$$g'(b) = \frac{-I^2 \partial_b \partial_N I - \partial_N I \partial_b \partial_N I + \partial_b I \partial_N^2 I + 2I \partial_b I \partial_N I}{I^2(I^2 + \partial_N I)}.$$

The denominator is positive, so we conclude the proof if we prove that the numerator is also positive.

$$\begin{aligned} g'(b)I^2(I^2 + \partial_N I) &= - \left(\int_0^\infty v(s) ds \right)^2 \left(bN \int_0^\infty u(s) ds - \int_0^\infty w(s) ds \right) \\ &\quad + b \int_0^\infty w(s) ds \left(bN \int_0^\infty u(s) ds - \int_0^\infty w(s) ds \right) \\ &\quad - Nb^2 \int_0^\infty w(s) ds \int_0^\infty u(s) ds + 2Nb \int_0^\infty v(s) ds \left(\int_0^\infty w(s) ds \right)^2 \\ &= -b \int_0^\infty v(s) ds \int_0^\infty u(s) ds + \left(\int_0^\infty v(s) ds \right)^2 \int_0^\infty w(s) ds + b \left(\int_0^\infty w(s) ds \right)^2, \end{aligned}$$

where in the first and last terms we have used the equality $N = I^{-1} = \left(\int_0^\infty v(s) ds \right)^{-1}$. It can be easily seen by observing the sign of the different parameters, the only negative term is the last one, so that though the following Cauchy-Schwarz inequality

$$\int_0^\infty v(s) ds \int_0^\infty u(s) ds \geq \left(\int_0^\infty w(s) ds \right)^2, \quad \text{as } w(s) = \sqrt{v(s)u(s)},$$

we cancel the last term with the first one and show that $\frac{d}{db} \partial_N f(b, N(b)) > 0 \forall b < 0$. \square

Acknowledgments

The authors acknowledge support from projects of the Spanish Ministerio de Ciencia e Innovación and the European Regional Development Fund (ERDF/FEDER) through grants PID2020-117846GB-I00, RED2022-134784-T, and CEX2020-001105-M, all of them funded by MCIN/AEI/10.13039/501100011033.

References

- [1] A. V. Rangan, G. Kovačič, and D. Cai. Kinetic theory for neuronal networks with fast and slow excitatory conductances driven by the same spike train. *Physical Review E*, 77(041915):1–13, 2008.
- [2] María J Cáceres, José A Carrillo, and Louis Tao. A numerical solver for a nonlinear Fokker–Planck equation representation of neuronal network dynamics. *Journal of Computational Physics*, 230(4):1084–1099, 2011.
- [3] Benoit Perthame and Delphine Salort. On a voltage-conductance kinetic system for integrate and fire neural networks. *Kinetic and related models, AIMS*, 6(4):841–864, 2013.
- [4] Benoît Perthame and Delphine Salort. Derivation of a voltage density equation from a voltage-conductance kinetic model for networks of integrate-and-fire neurons. *Communications in Mathematical Sciences*, 17(5), 2019.
- [5] K. Newhall, G. Kovačič, P. Kramer, A. V. Rangan, and D. Cai. Cascade-induced synchrony in stochastically driven neuronal networks. *Physical Review E*, 82:041903, 2010.
- [6] K. Newhall, G. Kovačič, P. Kramer, D. Zhou, A. V. Rangan, and D. Cai. Dynamics of current-based, poisson driven, integrate-and-fire neuronal networks. *Communications in Mathematical Sciences*, 8:541–600, 2010.
- [7] A Omurtag, Knight B. W., and L. Sirovich. On the simulation of large populations of neurons. *Journal of Computational Neuroscience*, 8:51–63, 2000.
- [8] G. Dumont and J. Henry. Synchronization of an excitatory integrate-and-fire neural network. *Bulletin of mathematical biology*, 75(4):629–648, 2013.
- [9] Grégory Dumont and Jacques Henry. Population density models of integrate-and-fire neurons with jumps: well-posedness. *Journal of Mathematical Biology*, 67(3):453–481, 2013.
- [10] Grégory Dumont and Pierre Gabriel. The mean-field equation of a leaky integrate-and-fire neural network: measure solutions and steady states. *Nonlinearity*, 33(12):6381, 2020.
- [11] K. Pakdaman, B. Perthame, and D. Salort. Dynamics of a structured neuron population. *Nonlinearity*, 23:55–75, 2010.
- [12] Khashayar Pakdaman, Benoît Perthame, and Delphine Salort. Relaxation and self-sustained oscillations in the time elapsed neuron network model. *SIAM Journal on Applied Mathematics*, 73(3):1260–1279, 2013.
- [13] Khashayar Pakdaman, Benoit Perthame, and Delphine Salort. Adaptation and fatigue model for neuron networks and large time asymptotics in a nonlinear fragmentation equation. *The Journal of Mathematical Neuroscience (JMN)*, 4(1):1–26, 2014.

- [14] Julien Chevallier, María José Cáceres, Marie Doumic, and Patricia Reynaud-Bouret. Microscopic approach of a time elapsed neural model. *Mathematical Models and Methods in Applied Sciences*, 25(14):2669–2719, 2015.
- [15] Julien Chevallier. Mean-field limit of generalized Hawkes processes. *Stochastic Processes and their Applications*, 127(12):3870–3912, 2017.
- [16] JA Acebrón, AR Bulsara, and W J Rappel. Noisy Fitzhugh-Nagumo model: From single elements to globally coupled networks. *Physical Review E*, 69(2):026202, 2004.
- [17] Stéphane Mischler, Cristóbal Quininao, and Jonathan Touboul. On a kinetic Fitzhugh–Nagumo model of neuronal network. *Communications in Mathematical Physics*, 342(3):1001–1042, 2016.
- [18] Richard Fitzhugh. Impulses and physiological states in theoretical models of nerve membrane. *Biophysical journal*, 1(6):445–466, 1961.
- [19] L. Lapicque. Recherches quantitatives sur l’excitation électrique des nerfs traitée comme une polarisation. *J. Physiol. Pathol. Gen*, 9:620–635, 1907.
- [20] L. Sirovich, A Omurtag, and Lubliner K. Dynamics of neural populations: Stability and synchrony. *Network: Computation in Neural Systems*, 17:3–29, 2006.
- [21] Nicolas Brunel. Dynamics of sparsely connected networks of excitatory and inhibitory spiking neurons. *Journal of computational neuroscience*, 8(3):183–208, 2000.
- [22] R. Brette and W. Gerstner. Adaptive exponential integrate-and-fire model as an effective description of neural activity. *Journal of neurophysiology*, 94:3637–3642, 2005.
- [23] Nicolas Brunel and Vincent Hakim. Fast global oscillations in networks of integrate-and-fire neurons with low firing rates. *Neural computation*, 11(7):1621–1671, 1999.
- [24] María J Cáceres, José A Carrillo, and Benoît Perthame. Analysis of nonlinear noisy integrate & fire neuron models: blow-up and steady states. *The Journal of Mathematical Neuroscience*, 1(1):7, 2011.
- [25] José A Carrillo, María d M González, Maria P Gualdani, and Maria E Schonbek. Classical solutions for a nonlinear Fokker-Planck equation arising in computational neuroscience. *Communications in Partial Differential Equations*, 38(3):385–409, 2013.
- [26] Maria J Cáceres and Benoît Perthame. Beyond blow-up in excitatory integrate and fire neuronal networks: refractory period and spontaneous activity. *Journal of theoretical biology*, 350:81–89, 2014.
- [27] María J Cáceres and Ricarda Schneider. Blow-up, steady states and long time behaviour of excitatory-inhibitory nonlinear neuron models. *Kinetic & Related Models*, 10(3):587, 2017.

- [28] María J Cáceres and Ricarda Schneider. Analysis and numerical solver for excitatory-inhibitory networks with delay and refractory periods. *ESAIM: Mathematical Modelling and Numerical Analysis*, 52(5):1733–1761, 2018.
- [29] María J Cáceres, Pierre Roux, Delphine Salort, and Ricarda Schneider. Global-in-time solutions and qualitative properties for the NNLIF neuron model with synaptic delay. *Communications in Partial Differential Equations*, 44(12):1358–1386, 2019.
- [30] Jingwei Hu, Jian-Guo Liu, Yantong Xie, and Zhennan Zhou. A structure preserving numerical scheme for Fokker-Planck equations of neuron networks: Numerical analysis and exploration. *Journal of Computational Physics*, 433:110195, 2021.
- [31] Pierre Roux and Delphine Salort. Towards a further understanding of the dynamics in the excitatory NNLIF neuron model: Blow-up and global existence. *Kinetic & Related Models*, 14(5), 2021.
- [32] Kota Ikeda, Pierre Roux, Delphine Salort, and Didier Smets. Theoretical study of the emergence of periodic solutions for the inhibitory NNLIF neuron model with synaptic delay. *Mathematical Neuroscience and Applications*, (4):1–37, 2022.
- [33] François Delarue, James Inglis, Sylvain Rubenthaler, Etienne Tanré, et al. Global solvability of a networked integrate-and-fire model of McKean–Vlasov type. *The Annals of Applied Probability*, 25(4):2096–2133, 2015.
- [34] François Delarue, James Inglis, Sylvain Rubenthaler, and Etienne Tanré. Particle systems with a singular mean-field self-excitation. Application to neuronal networks. *Stochastic Processes and their Applications*, 125(6):2451–2492, 2015.
- [35] Jian-Guo Liu, Ziheng Wang, Yuan Zhang, and Zhennan Zhou. Rigorous justification of the Fokker–Planck equations of neural networks based on an iteration perspective. *SIAM Journal on Mathematical Analysis*, 54(1):1270–1312, 2022.
- [36] Alfonso Renart, Nicolas Brunel, and Xiao-Jing Wang. Mean-field theory of irregularly spiking neuronal populations and working memory in recurrent cortical networks. *Computational neuroscience: A comprehensive approach*, pages 431–490, 2004.
- [37] María J. Cáceres and Alejandro Ramos-Lora. An understanding of the physical solutions and the blow-up phenomenon for nonlinear noisy leaky integrate and fire neuronal models. *Communications in Computational Physics*, 30(3):820–850, 2021.
- [38] M. J. Cáceres. A review about nonlinear noisy leaky integrate and fire models for neural networks. *Rivista di Matematica della Università di Parma*, 2:269–298, 2019.
- [39] Xu’an Dou and Zhennan Zhou. Dilating blow-up time: A generalized solution of the NNLIF neuron model and its global well-posedness. *arXiv preprint arXiv:2206.06972*, 2022.

- [40] José Carrillo, Benoît Perthame, Delphine Salort, and Didier Smets. Qualitative properties of solutions for the noisy integrate & fire model in computational neuroscience. *Nonlinearity*, 25:3365–3388, 2015.
- [41] José A Cañizo and Havva Yoldaş. Asymptotic behaviour of neuron population models structured by elapsed-time. *Nonlinearity*, 32(2):464, 2019.
- [42] Delphine Salort and Didier Smets. Convergence towards equilibrium for a model with partial diffusion. *Communications in Partial Differential Equations*, pages 1–19, 2024.
- [43] María J Cáceres, José A Cañizo, and Alejandro Ramos-Lora. On the asymptotic behavior of the NNLIIF neuron model for general connectivity strength. *arXiv preprint arXiv:2401.13534*, 2024.
- [44] Ziyu Du, Yantong Xie, and Zhennan Zhou. A synchronization-capturing multi-scale solver to the noisy integrate-and-fire neuron networks. *Multiscale Modeling & Simulation*, 22(1):561–587, 2024.
- [45] Pei Zhang, Yanli Wand, and Zhennan Zhou. A spectral method for a fokker-planck equation in neuroscience with applications in neuron networks with learning rules. *Communications in Computational Physics*, 35(1):70–106, 2024.
- [46] Bernardo Cockburn, Chi-Wang Shu, Claes Johnson, Eitan Tadmor, and Chi-Wang Shu. *Essentially non-oscillatory and weighted essentially non-oscillatory schemes for hyperbolic conservation laws*. Springer, 1998.